Self-healing Network Architectures for Multiwavelength Optical Metro/Access Networks

SUN Xiaofeng

A Thesis Submitted in Partial Fulfilment

of the Requirements for the Degree of

Master of Philosophy

in

Information Engineering

February 2006

Acknowledgement

First of foremost, I would like to express my deepest gratitude to my thesis supervisor, Prof. Chun-Kit Chan, for his continuous support and guidance in my research. Throughout my postgraduate studies, he has taught me a lot of research methods and experimental skills which are invaluable for my work. His scholarship and sincerity towards research has always been inspirational to me. He has in-depth knowledge in many areas of optical communications. Discussions with him have always been fruitful and have inspired many research ideas which eventually led to this thesis. His advices have also been very instrumental to my experimental work and paper writing. I would also like to thank Prof. Lian-Kuan Chen and Prof. Chinlon Lin for their continuous support and guidance.

Throughout my studies, I am fortunate to be able to work alongside many talented fellow postgraduate students in Lightwave Communications Laboratory in the Department of Information Engineering. In particular, I would like to thank Mr. Chi-Man Lee and Mr. Zhaoxin Wang for their helpful discussions and technical support. I would also like to express my appreciation to lab members including Dr. Li Huo, Dr. Guowei Lu, Mr. Ning Deng, Mr. Yuen-Ching Ku, Mr. Jian Zhao, Mr. Siu-Ting Ho, Mr. Siu-sun Pun, Mr. Bo Zhang, and Mr. Qiguang Zhao.

Abstract

In recent years, with the rapid growth of the Internet, the bandwidth demand for data traffic has ever been exploding. Optical networks based on wavelength-division multiplexing (WDM) technology are promising to offer cost-effective access of high-bandwidth data to satisfy the bandwidth requirements of the Internet infrastructure. However, with the possible occurrence of fiber cuts and the tremendous traffic loss a failure may cause, network survivability and fault management becomes critical concerns in network design and real-time operation. In this thesis, protection and self-healing network architectures for WDM metro and access networks, are designed and demonstrated to enhance the network survivability.

In the arena of access networks, multi-wavelength passive optical networks (WDM-PON) are emerging to deliver broadband services. Thus, reliable access network architecture is highly desirable. In this thesis, we propose two self-healing network architectures for WDM-PON, which provides protection against link failure between the remote node (RN) and the optical network units (ONUs), as well as that between the RN and the optical line terminal (OLT).

In metro access network arena, WDM self-healing ring (SHR) networks are promising to ensure network reliability. In order to reduce the system cost and to increase the fiber efficiency in SHR networks, we propose a new single-fiber bi-directional WDM SHR metro-access ring network with simple B-OADMs. An alternate-path switching scheme is designed for protection against any single fiber failure in the network.

Nowadays, networks are migrating from SONET rings to mesh topology because of the poor scalability of interconnected rings and the excessive resource redundancy used in ring-based fault management schemes. In this thesis, we propose a new mesh self-healing network architecture. An all-optical deflection routing scheme is designed not only to protect against the fiber failure on the physical layer, but also highly enhance the scalability of the network. The proposed network will also be experimentally investigated in this thesis.

In general, the above proposed self-healing networks architectures can achieve prompt traffic restoration under fiber link failures. The proposed protection mechanisms are mainly performed in the optical layer, thus they can simplify and facilitate the network management.

摘要

近年來，隨著互聯網（Internet）的快速發展，數據業務對帶寬的要求也呈爆炸式增長。基於波分複用（WDM）的多波長光纖網絡爲滿足互聯網帶寬要求提供了一個有效的解決方案。爲了增強網絡的容錯和自我恢復能力，網絡需要具備實用的保護結構，從而使得網絡物理層的故障可以在很短時間內恢復，降低數據丟失的可能性。本論文提出並討論了用於光接入網和光城域網方面的保護結構，來實現網絡保護和業務數據的恢復。

在光接入網方面，多波長無源光網絡（WDM-PON）爲寬帶互動式業務提供了一個有效的解決方案。網絡的可靠性和自動保護倒換功能是系統設計者要面對的一個巨大挑戰。在本論文中，我們提出了兩種新的具備保護能力的光接入網絡結構。第一個結構實現了在樹狀-環形混合網絡中的自動保護功能，而第二個結構實現了樹狀網絡中的自動保護。通過採用以上的保護結構，受影響的數據業務可以被自動地重新路由，並且網絡中的任何光纖故障將對光纖路終端（OLT）透明。利用陣列波導光柵（AWG）的週期譜特性和合理的波長路由技術，可以實現基於鏈路的自動保護。

在光城域接入網方面，多波長自愈合環網大大增強了網絡的可靠性。另一方面爲了進一步降低系統成本和增加光纖利用效率，我們在本論文中提出了一種新型的單光纖雙向多波長自愈合環網結構，並且設計了相應的雙向光上下路複用器（B-OADM）。利用環網路由倒換策略，被任何光纖故障影響的數據可以快速自我恢復。

在光城域網方面，由於環形拓撲結構難於拓展以及綫路利用率低，網狀拓撲將成爲下一代城域網絡的主要結構。在本論文中，我們提出了一種新型的網狀拓撲自愈合網絡，並且提出了全光偏向路由機制。在網絡的物理層上實現了對光纖故障的保護機制，而且大大提高了網絡的可擴展性。

Table of Contents

List of Figures

List of Tables

Chapter 1
Introduction

1.1 Optical network evolution

The recent explosive growth of the Internet has created enormous potential for fiber optic communication systems. Today, various optical fiber systems, exploiting their inherent advantages dominate in different segments of communication infrastructure. They are usually characterized by geographical reach. The topology of a typical modern communication network is shown in Fig. 1.1.

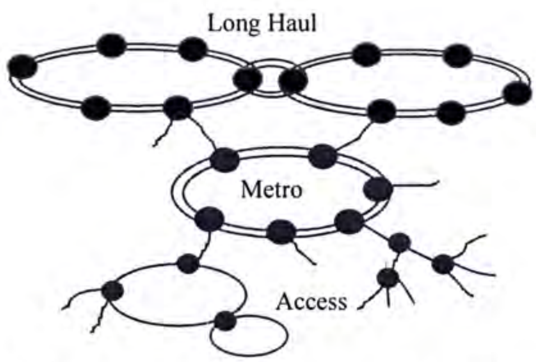

Fig. 1.1 Schematic of the fibre network infrastructure

The core of the infrastructure consists of transoceanic submarine links and long haul terrestrial links operating at 1550nm wavelength window on single mode fiber. Metro backbone and metro access links connect to business enterprise and residential users.

Access networks within business and academic environments heavily use fiber optic systems in network backbones. The recent introduction of Gigabit Ethernet standard has accelerated the deployment of fiber systems in the access network and hence faster fiber systems will be the core infrastructure.

1.1.1 Submarine and terrestrial long-haul fibre systems

Submarine and long-haul terrestrial fiber systems use the 1550nm-wavelength window, allowing greater repeater spans due to the minimum loss of the fiber in this region. The EDFAs are used with typical spans of 80 km. Dispersion compensation techniques are usually deployed along the link using dispersion compensating fibers or fiber gratings [1].

Wavelength Division Multiplexing (WDM) offers a tremendous increase in long-haul terrestrial and submarine link capacity by effectively increasing the capacity of fiber optical cables. Optical amplifiers in the link are shared by all the wavelengths reducing the cost of the link considerably.

Submarine optical fiber links have used WDM technology to increase the capacity by many times. A few recently deployed transoceanic submarine optical fiber links are given in the Table 1.1 [1].

Name	Destination Countries	Distance (km)	Aggregate Data rate (Gbit/s)	Commissi-oned year
SEA-ME-WE-3	Germany-China	38000	5Gbit/s	1998
Gemini (South/North)	USA-UK	6260/5855	60Gbit/s WDM	1998
Mid-Atlantic Crossing (MAC)	USA-Caribbean	9400	20Gbit/s WDM	1999
Pacific Crossing-1 (PC-1)	USA-Japan	21000	80Gbit/s	2000
Atlantic-1 (FLAG)	USA-UK-France	12570	80Gbit/s DWDM	2000/2001

Table 1.1 Recent optical fiber submarine cable systems

SEA-ME-WE 3, which is owned by 34 operators, connects 40 stations from Australia and Japan to Northern Europe through the Middle East [1]. It carries 8 wavelengths on each of two fiber pairs. Gemini consists of a transatlantic undersea ring and two terrestrial rings in the US and UK [2].

Until recently powerful telecom operators dominated the ownership of submarine cables. Estimates have shown that most transatlantic cables paid for themselves within three years or less, despite an expected lifetime of 25 years [3]. The advent of telecom deregulation has brought competition to the submarine network business. A new wave of telecom operators and operators who transport other operator's traffic (carriers' carriers) are emerging [2]. New opportunities have been created enabling direct optical links between major cities of the world.

Submarine systems are evolving from point-to-point links to complex high-capacity networks [4]. The latest transoceanic systems have a capacity of up to 40 Gb/s per fiber pair compared to the first fiber optic cable laid across Atlantic (TAT-8) providing a maximum bandwidth of 280 Mbit/s per fiber pair [5].

1.1.2 Metropolitan networks

The dynamics of long-haul and metropolitan applications are different. The long haul focuses on adding more bandwidth while reducing the cost per mile, short-haul applications require much more flexibility due to the need to deliver a broader range of services and to easily add new customers on the network. Metropolitan and access optical fiber systems mainly consist of unamplified links operating at 1300nm/1550nm wavelength window [6]. Fig. 1.2 shows different type of customers in the metropolitan network environment [7].

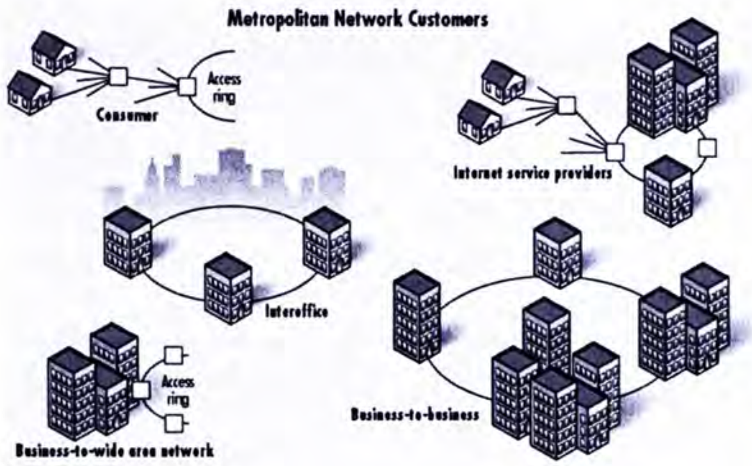

Fig. 1.2 Metropolitan networks connect to variety of users each with specific networking requirement [7]

Driven by falling costs and increasing penetration in the long-haul sector, WDM is now beginning to migrate toward the metro-networks area. When the initial wave of enterprise optical backbones reaches fiber exhaustion, the demand on WDM solutions in metropolitan networks will increase. Other possibilities being a major network user with high bandwidth requirements might link its buildings. Data centers (banks and other financial institutions) are possible customers.

1.1.3 Access networks

The data traffic of the Internet has grown faster than predicted in the last decade. Traffic on the Internet is reported as doubling every three months [8]. Higher bandwidth demand from the local area networks has introduced more fiber optic technology in this area. Data communication systems demand low cost optical components.

A number of high-speed optical data communication standards are already established in the LAN environment. The Fiber Distributed Data Interface (FDDI) was introduced as a backbone standard using a ring topology at 125Mb/s rate [9]. The standard physical layer specifies 1300nm LEDs as light sources and 62.5um multi-mode fiber transmission medium supporting 200 km of fiber path per network, with individual links spanning up to 2 km. Fiber channel is a standard developed mainly for high-speed data transfer between computers and data storage systems. It is also being used in server backbones and connecting other fast peripherals to computers. The ability to access mass storage devices quicker and from greater distances is very attractive to applications like multimedia, medical imaging and CAD applications. Fiber channel will most likely continue to expand into storage markets [9].

Ethernet is the most widely used local area network standard in the world today [6]. It has evolved from initial 10Mb/s Ethernet to Fast Ethernet. Fast Ethernet uses multimode fiber for building and campus backbone links. Unshielded Twisted Pair (UTP) cabling is mainly used in horizontal cabling. The physical transmission media used for Fast Ethernet standard are shown in Table 1.2.

	Transmission medium	Signal type	Max. link length
100Base-TX	UTP	Electrical	100 m
100Base-FX	Multi Mode Fiber	1300nm optical	2 km

Table 1.2 Fast Ethernet (100Mbs) IEEE802.3u

Recently Gigabit Ethernet has been introduced to increase the bandwidth in local area networks as a result of vast deployment of Ethernet technology. The need for higher bandwidth technologies being backward compatible has resulted in Gigabit Ethernet emerging as an industry standard for high-speed local area networking. Initially, Gigabit Ethernet is expected to be deployed in backbones in existing networks. However in the future, with the advent of faster and more powerful desktop computers, high bandwidth, time-sensitive services will be able to provide for local area network end users.

Gigabit Ethernet specifications for physical transmission media are given in Table 1.3.

Transmission Medium	Signal type	Max. Link length
UTP1	Electrical	25 m
62.5/125 μm fiber	850nm optical	220/275 m
50/125 μm fiber	850nm optical	500/550 m
50/125 μm fiber	1300nm optical	550 m
62.5/125 μm fiber	1300nm optical	550 m
9/125 μm fiber	1300nm optical	5 km

Table 1.3 Gigabit Ethernet (1000Mbs) IEEE802.3z

With the ten-fold increase in the data rate from fast Ethernet to Gigabit Ethernet, single mode fiber technology has emerged into the local area network environment for the first time. Short wavelength sources no longer can support campus backbone link distances resulting in campus backbone links being implemented using single mode fiber.

Gigabit Ethernet has become a competitor to well established Asynchronous Transfer Mode (ATM) technology in some areas of networking industry. Being a cost effective and natural extension to existing Ethernet technology, Gigabit Ethernet provides smooth and relatively simple network upgrades to faster data rates. The main advantage of ATM over Gigabit Ethernet is the quality of service (QoS) [10]. ATM is specially designed to integrate telephony, data, and video traffic on one network accommodating a variety of bit rates. However the Ethernet technology along with DWDM technology is merging to provide new form of services with high QoS [10].

The next stage of Ethernet evolution is already taking place, as the 10 Gigabit Ethernet proposal is under consideration by the IEEE 802.3 standards-making committee [11][12]. Four optical technologies are now under consideration for 10Gbit/s Ethernet. They are, serial 10Gbit/s, four channel WDM (4x2.5Gbit/s line rate), parallel optics and multi-level analogue signaling. Serial 10Gbit/s links could run to 300m on 50um diameter multimode fiber, using either 850nm or 980nm VCSELs though 62.5um is the predominant installed base. Single mode variants could provide a range of connectivities: 2 km spans using directly modulated, uncooled 1300nm Fabry-Perot lasers without external isolator over single mode fiber; 10 km spans using directly modulated, uncooled 1300nm DFB lasers with no external isolator; or 40 km spans using externally modulated, uncooled 1300nm DFB lasers with optical isolators. 10Gbit/s Ethernet will undoubtedly converge datacom technologies even more in local, metropolitan and wide-area applications in the future.

1.2 Motivation of this thesis

As the optical networks evolve from today's technology (SDH-based) towards the future all-optical technology, and with the implementation of wavelength-division multiplexing technology in metro and access networks, the failure of network elements (e.g., fiber links) may cause the failure of several optical channels, thereby leading to large data losses. Although higher protocol layers such as asynchronous transfer mode (ATM) and Internet protocol (IP) have recovery procedures to recover from link failures, the recovery time is still significantly large (on the order of seconds), whereas restoration times at the optical layer will be on the order of a few milliseconds to minimize data losses. Furthermore, survivability at the optical layer provides protection to higher layer protocols that may not have built-in protection. Thus, fast and reliable optical protection architectures are highly desired.

In this thesis, we propose several self-healing network architectures for multiwavelength optical metro/access networks. We investigate and experimentally demonstrate two self-healing networks – Star-Ring Protection Architecture and Duplicated-Tree Protection Architecture – for multiwavelength optical access network. The traffic can be restored promptly under both feeder and distribution fiber link failures, as well as the AWG failure at the RN simultaneously. We also propose a single-fiber bi-directional self-healing WDM ring for optical metro access networks. Each access node (AN) is incorporated with a simple low-cost bidirectional optical add-drop multiplexer (B-OADM) for adding/dropping wavelength channels to/from the hub node. The proposed ring network can realize traffic restoration without the need of an extra protection fiber nor doubling the number of optical transceivers. Moreover, we propose a new protection architecture for mesh metro backbone networks. The network design and the protection strategies under various fiber failure scenarios will be discussed. The experiment results confirm the feasibility of the proposed network architecture.

1.3 Outline of this thesis

The organization of the remaining chapters of this thesis will be as followings:

Chapter 2: Previous protection architectures will be outlined. Traditional protection architectures for TDM-PON and recent protection architectures for access networks will be reviewed. Then recently proposed self-healing network architectures for metro access networks will be discussed. In the end, traditional self-healing ring architectures (SONET based) in metro backbone networks will be reviewed.

Chapter 3: Two novel self-healing network architectures for multiwavelength optical access networks will be proposed. One is called Star-Ring Protection Architecture (SRPA) and the other is called Duplicated-Tree Protection Architecture (DTPA). By using the wavelength routing property of the AWG in the RN, fast and automatic protection switching without interference to normal traffic is achieved.

Chapter 4: Self-healing network architectures for metro access networks will be discussed. A Single-Fiber Bi-directional WDM self-healing ring network with simple and low-cost bi-directional OADM will be proposed. By employing our proposed alternate-path switching scheme, the bi-directional traffic can be restored promptly under any single fiber failure.

Chapter 5: A novel self-healing WDM mesh architecture for metro backbone networks will be proposed. With a unified network node design, an all-optical deflection routing scheme is proposed to realize bi-directional fiber link restoration for mesh metro backbone network.

Chapter 6: Summary and future works.

Chapter 2
Previous Self-Healing Network Architectures

2.1 Introduction

Traffic protection functionality can be implemented in different layers of a functional mode, either in the electrical layer or in the optical layer. Network protection can be implemented electrically in the Path or Multiplex Section (MS) layers of the SDH, or optically in the OC or Optical Multiplex Section (OMS) layers of the optical architecture. The implementation can also be of the dedicated or shared type. In the first case an alternative route has its full capacity dedicated to protection of the main route. In the second case, the capacity of two different routes is shared between service traffic and protection traffic, none of the routes being dedicated to protection or service.

As the optical networks evolve from today's technology (SDH-based) towards the future all-optical technology, and with the implementation of wavelength-division multiplexing technology in metro and access networks, the failure of network elements (e.g., fiber links) may cause the failure of several optical channels, thereby leading to large data losses. Although higher protocol layers such as asynchronous transfer mode (ATM) and Internet protocol (IP) have recovery procedures to recover from link failures, the recovery time is still significantly large (on the order of seconds), whereas restoration times at the optical layer will be on the order of a few milliseconds to minimize data losses. Furthermore, survivability at the optical layer provides protection to higher layer protocols that may not have built-in protection. Thus, fast and reliable optical protection architectures are highly desired.

2.1.1 Previous protection architectures for access networks

Most optical access networks employ point-to-multipoint network topology. The physical layer is shared. The major cause of network downtime is fiber breaks. To improve the availability, some fiber sections have to be duplicated. The ITU-T Recommendation on PON (G.983.1) [13] have suggested four possible fiber duplication and protection switching scenarios, as shown in Fig. 2.1, though they were regarded as optional protection mechanisms. Note that the RN only comprises 1×N optical power splitter(s) in ITU-T G.983.1, but those protection architectures can also be applied to multi-wavelength PON by replacing the optical power splitters by wavelength demultiplexers.

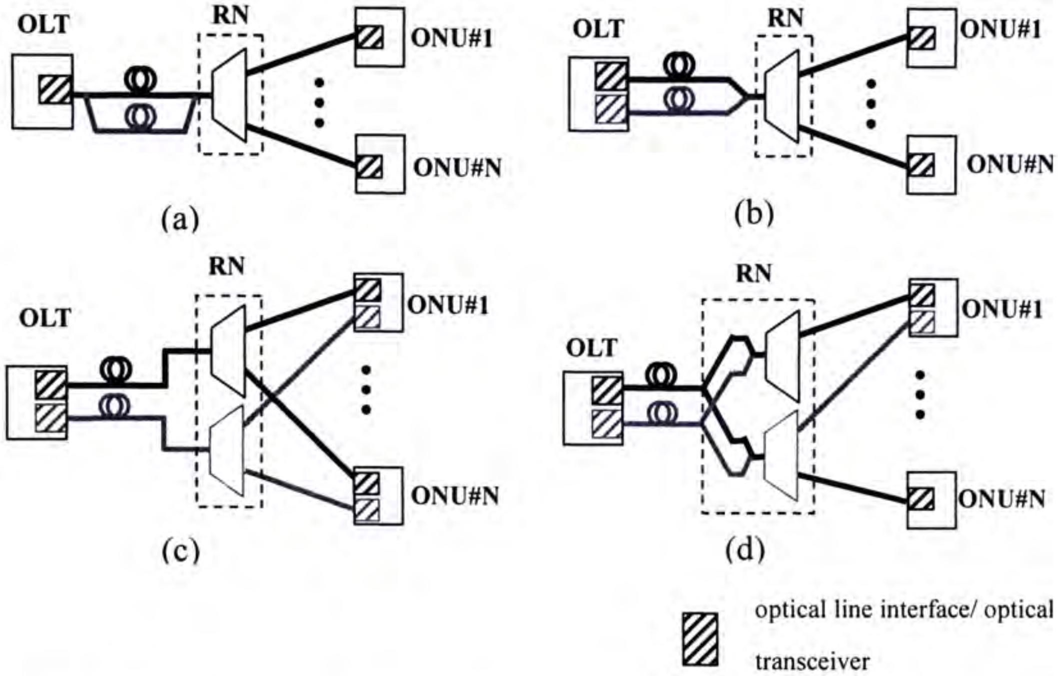

Fig. 2.1 Protection switching architectures suggested by ITU-T G.983.1

Fig. 2.1 shows the four suggested protection architectures with different levels of protection. Fig. 2.1(a) duplicates the fiber feeder between the OLT and the RN only. Fig. 2.1(b) doubles the optical transceivers at the OLT and also duplicates the fiber feeder between the OLT and the RN. Protection switching is done by switching the data to the backup optical transceiver at the OLT. Fig. 2.1(c) doubles not only the OLT side facilities but also the RN and the ONU sides. Failure at any point can be recovered by switching to the backup facilities. Fig. 2.1(d) incorporates an additional power splitter circuit to cope the case that not all ONUs have duplicate optical transceivers, due to some environmental constraints.

Recently, several protection architectures for WDM optical access networks have been proposed. In [14], a self-healing DWDM/SCM modified star-ring architecture was proposed, in which two adjacent RNs were connected by a ring, and each ring was connected with multiple ONUs. The overall architecture is shown in Fig. 2.2. The RN was incorporated with some protection switches so that in case of fiber cut between itself and the OLT, the traffic on both of its attached rings would be bypassed and forwarded to its adjacent RN so that the affected ONUs can still be in contact with the OLT. This special structure, in fact, is employed to eliminate the optical beat interference (OBI) problem due to subcarrier multiplexing. This architecture is a feasible choice in terms of the capacity, the OBI-reducing capability, the quality-of-service (QoS), and the cost of initial installation. But, this scheme still has many rooms for improvement. Complexity in scalability, inflexible topology without sufficient variations, and high equipment cost become some critical problems.

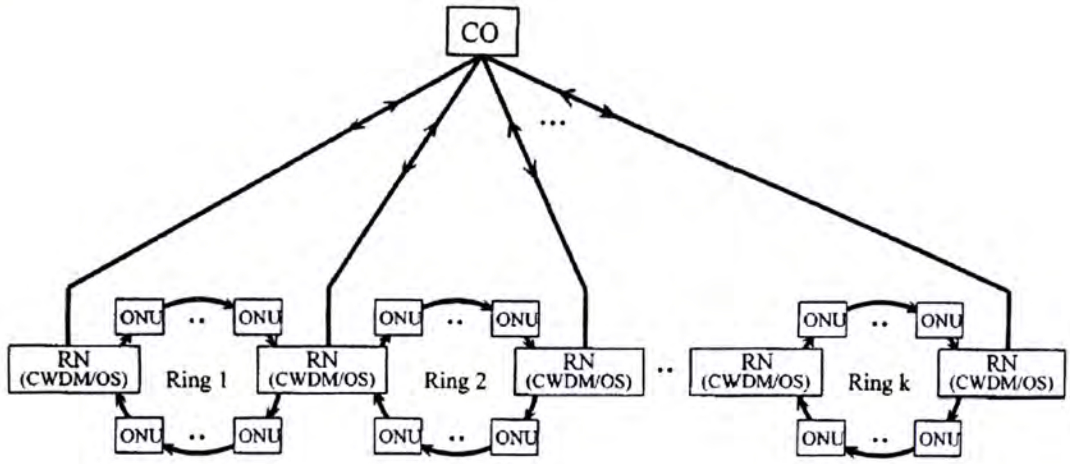

Fig. 2.2 Star-Ring-Bus architecture in access network [14]

In [15][16], a group protection architecture (GPA) for WDM-PON networks has been proposed, as illustrated in
Fig. 2.3. By employing a well-designed wavelength assignment scheme, it provides protection against fiber link failure between the RN and the ONUs.

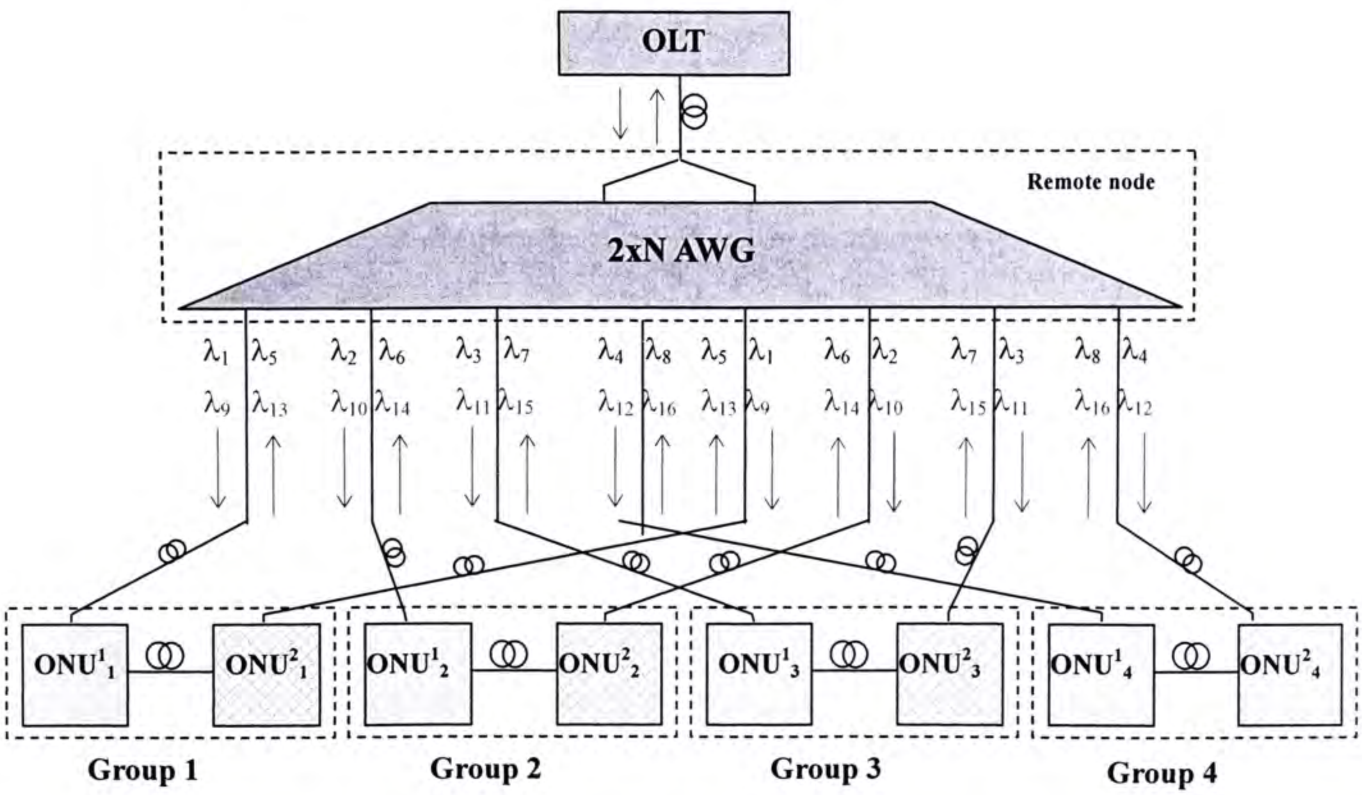

Fig. 2.3 Network topology of GPA scheme

The traffic in both downstream and upstream directions can be re-routed via the adjacent ONU, thus the optical line terminal (OLT) is transparent to such fiber failure and the affected ONU can still communicate with the OLT bi-directionally. However, this scheme only provides the protection against the fiber link failure between the RN and ONUs. A more reliable self-healing architecture for access network with protection capability against both the feeder and distribution fiber failures as well as the components failure in the RN is highly desired.

2.1.2 Previous protection architectures for metro access networks

In metro access networks, which connect the metro backbone networks and the access networks, the ring topology has been considered as a cost-effective survivable network architecture due to bandwidth sharing and improved survivability [17]. Most metro access networks work in a hub-access node architecture, traffic from many access nodes (ANs) or remote nodes (RNs) is transmitted/received to/from a hub node or central office (CO), and the hub node or central office controls the traffic between ANs.

In [18], a bidirectional WDM self-healing ring network composed of add and drop fibers was proposed, as illustrated in Fig. 2.4. Two-fiber ring connects a central office (CO) and N remote nodes (RNs). Each RN consists of two 2x2 optical switches, an AM module connected to the add fiber for adding the upstream signals bidirectionally and a DD module connected to the drop fiber for dropping the downstream signals bidirectionally.

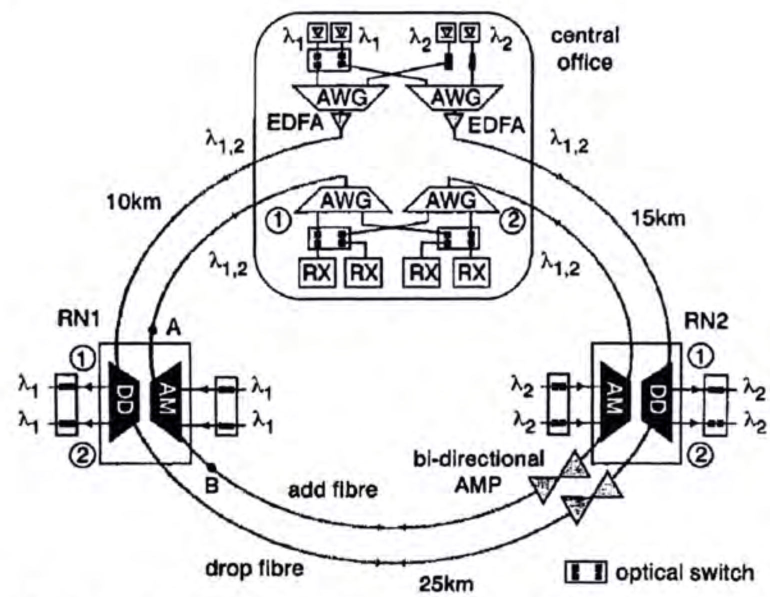

Fig. 2.4 Bidirectional WDM SHR network with add and drop fiber [18]

Under single fiber link failure, the 2x2 optical switch will change their state to exchange the paths of the bidirectional signals to ensure survival of the higher priority signal in the protection state. This network relaxes the device requirement for suppression of the relative intensity noise (RIN) in the bidirectional ring networks and the self-healing function is achieved without the need for protection switches in the transmission paths. However, this network requires two fibers which increase the implementation cost.

Recently, in order to further reduce the system cost and increase the fiber efficiency in SHR networks, single-fiber bi-directional SHR networks based on bi-directional optical add-drop multiplexer (B-OADM) [19][20] have recently attracted much research interest. In [19], a bidirectional WDM SHR with a single strand of fiber for metro access networks based on BADM for path-switched ring was proposed. The overall architecture is shown in Fig. 2.5. The CO and RNs were incorporated with some protection switches so that in case of fiber cut between the RN and the CO, the high priority traffic would be switched to the available path in the single fiber ring so that the affected RN can still be in contact with the CO.

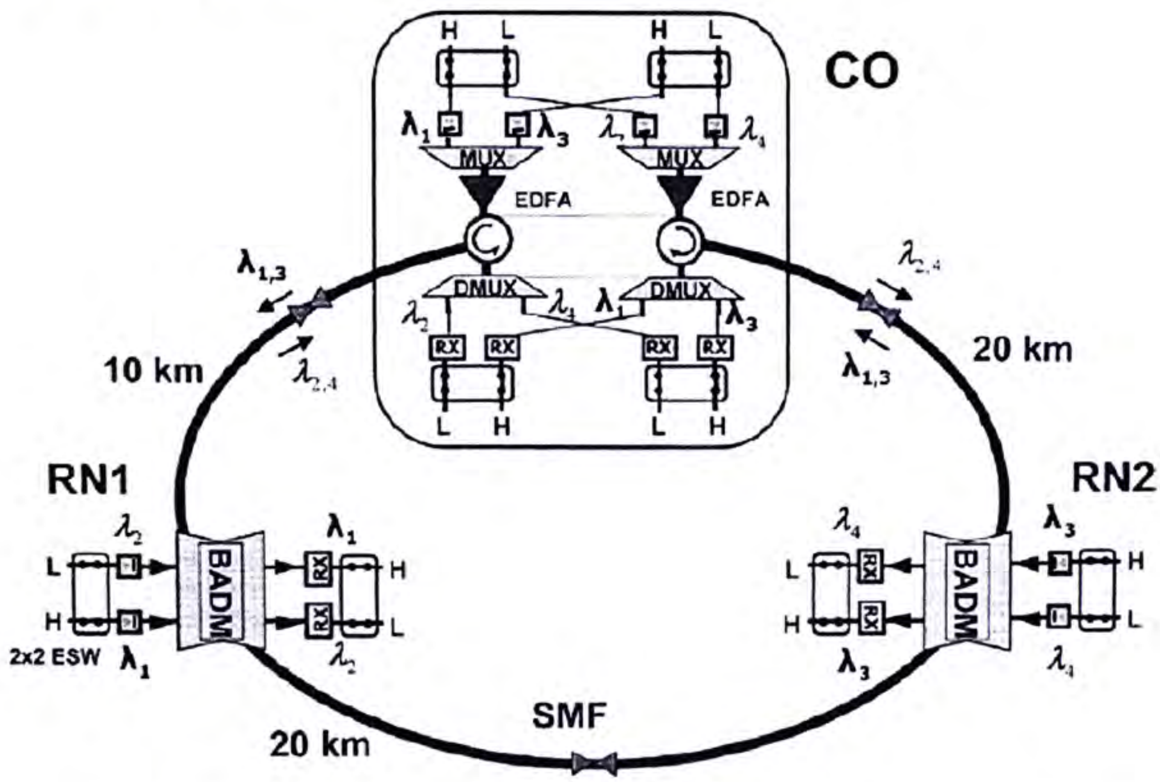

Fig. 2.5 Single-fiber bidirectional WDM SHR network architecture [19]

The proposed ring network can double the transmission capacity in the operating state and provide the self-healing function without protection in the transmission path. However, this scheme still has many rooms for improvement. Complexity in access node and high equipment cost become some critical problems.

2.3 Previous protection architectures for metro backbone networks

In metro backbone network, several self-healing ring architectures using electronic add-drop multiplexers (SONET ADMs) have been proposed for telecommunication applications. The network ring incorporates protection mechanisms that automatically detect failures and reroute traffic away from the failed links and nodes onto other routes rapidly. Unidirectional Path-switched Rings and Bi-directional Line-switched Rings are commonly used in the SONET ring networks for protection purpose. Interconnected rings and dual homing are some improved version. We will review those architectures in this section.

2.3.1 Unidirectional path-switched rings (UPSR)

UPSR can be viewed as 1+1 path protection at path layer [21]. One fiber is used as the working fiber and the other as the protection fiber. Traffic from node A to node B is sent simultaneously on the working fiber in the clockwise direction and on the protection fiber in the counter-clockwise direction. The protection is performed at the path layer for each connection as follows: Node B continuously monitors both the working and protection fiber and selects the better signal between the two for each SONET connection. Under normal operation, suppose node B receives traffic from the working fiber. If there is a link failure, say, of link AB, then B will switch over to the protection fiber and continue to receive the data.

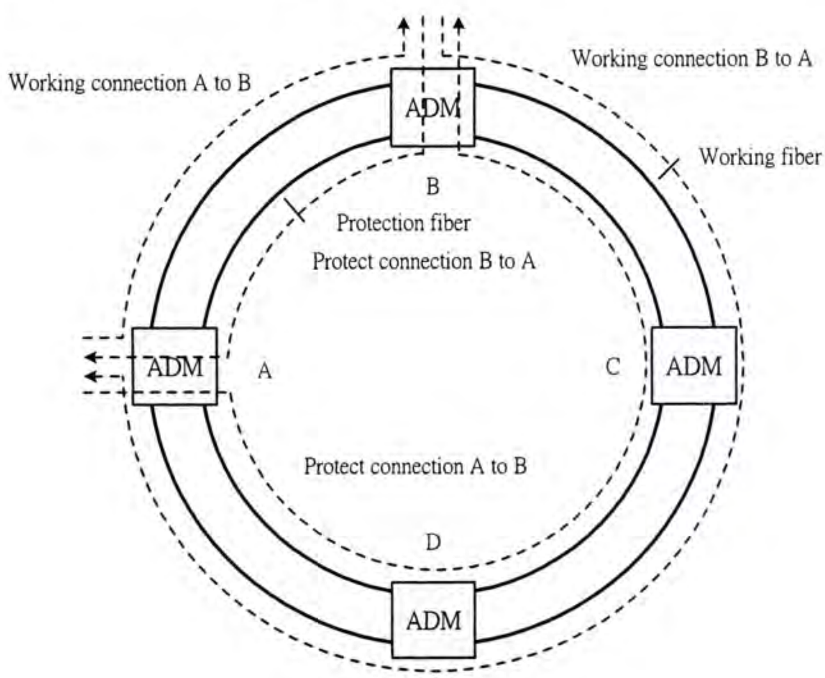

Fig. 2.6 Unidirectional path-switched rings. One of the fibers is considered the working fiber and the other the protection fiber. Traffic is transmitted simultaneously on the working fiber in the clockwise direction and on the protection fiber in the counterclockwise direction. Protection is done at the path layer.

2.3.2 Bidirectional line-switched rings (BLSR)

BLSRs are much more sophisticated than UPSRs and incorporate additional protection mechanisms [21]. Unlike a UPSR, they operate at the line or multiplex section layer. The BLSR equivalent in the SDH world is called a multiplex section shared protection ring (MS-SPRing). Unlike a UPSR, working traffic in a BLSR can be carried on both directions along the ring. For example, on the working fiber, traffic from node A to node B is carried clockwise along the ring, whereas traffic from B to A is carried counter clockwise along the ring. Usually, traffic belonging to both directions of a connection is routed on the shortest path between the two nodes in the ring. In case of a fiber or cable cut, service is restored by ring switching. Suppose link AB fails. The traffic on the failed link is then rerouted by nodes A and B around the ring on the protection fibers. Ring switching is also used to protect against a node failure.

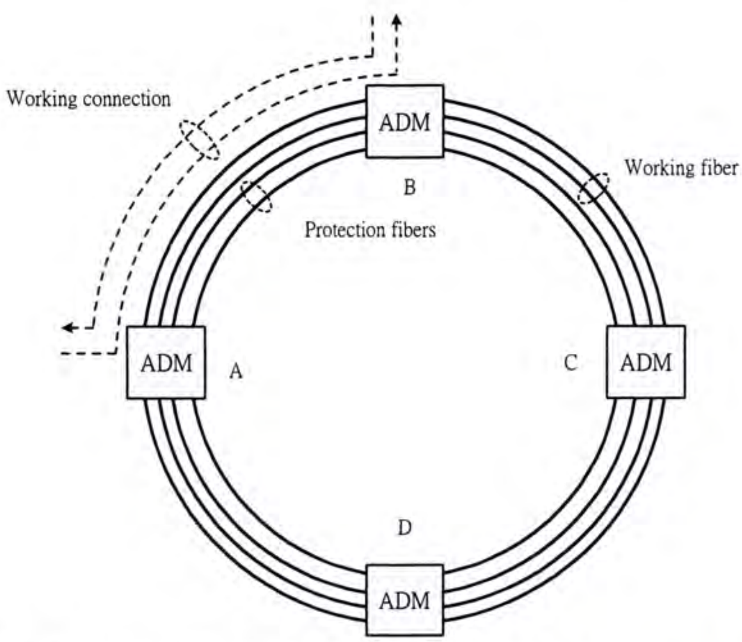

Fig. 2.7 A four bi-directional line-switched ring. The ring has two working fibers and two protection fibers. Traffic between two nodes is transmitted normally on the shortest path between them, and either span or ring switching is used to restore service after a failure.

BLSRs provide spatial reuse capabilities by allowing protection bandwidth to be shared between spatially separated connections. Thus BLSRs are more efficient than

UPSRs in protecting distributed traffic patterns. For this reason, BLSRs are widely deployed in long-haul and interoffice networks, where the traffic pattern is more distributed than in access networks.

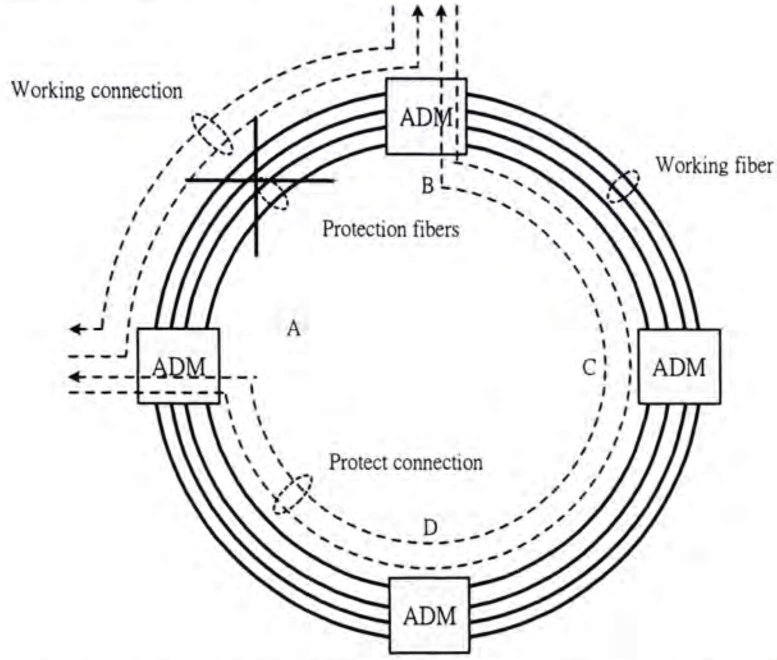

Fig. 2.8 Protection route in BLSR. Traffic is rerouted around the ring by the nodes adjacent to the failure

2.3.3 Ring interconnection and dual homing

Metro network is often made up of rings structure [21]. A single ring is only a part of the overall network. The entire network typically consists of multiple rings interconnected with each other, and a connection may have to be routed through multiple rings to get its destination. The simplest way for rings to interoperate is to connect the drop sides of two ADMs on different rings back to back.

Fig. 2.9 shows the one of the possible interconnection. One of the problems of this approach is that if one of the ADMs fails, or there is a problem with the cabling between the two ADMs, the interconnection is broken. A way to deal with this problem is to use dual homing.

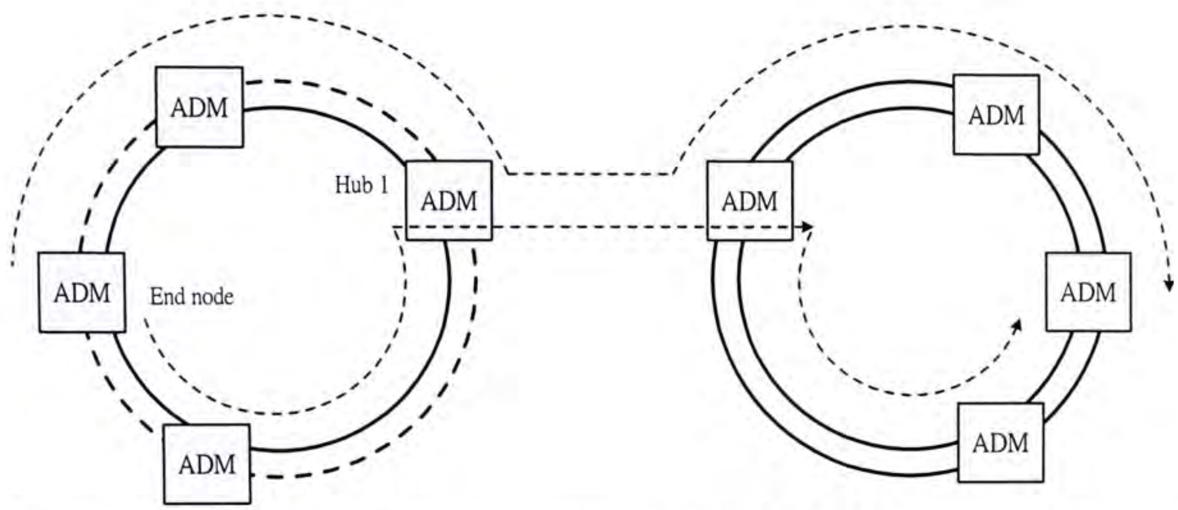

Fig. 2.9 Back-to-back interconnection of SONET/SDH rings. This simple interconnection is vulnerable to the failure of one of the two nodes that form the interconnection, or of the link between these two nodes.

Dual homing makes use of two hub nodes to perform the interconnection, as illustrated in Fig. 2.10. For traffic going between the rings, connections are set up between the originating node on one ring and both the hub nodes. Thus if one of the hub nodes fails, the other node can take over, and the end user does not see any disruption to traffic. Similarly, if there is a cable cut between the two hub nodes, alternate protection paths are now available to restore the traffic.

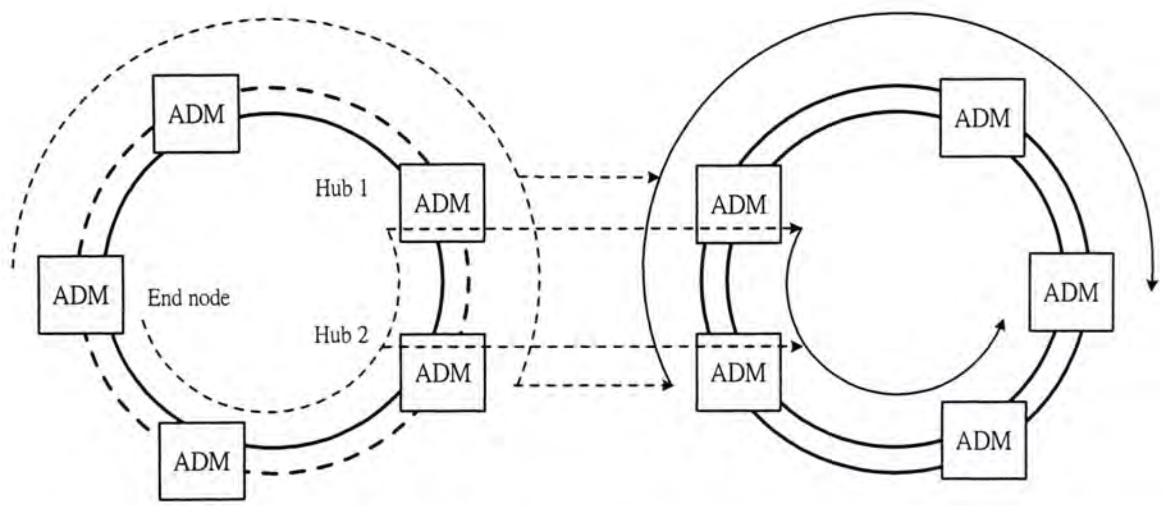

Fig. 2.10 Dual homing to handle hub node failures. Each end node is connected to two hub nodes so as to be able to recover from the failure of a hub node or the failure of any interconnection between the hub nodes. The add drop module (ADM) in the nodes have a “drop-and-continue” feature, which allows them to drop a traffic stream as well as have it continue onto the next add drop nodes.

2.4 Summary

In this chapter, previous protection architectures in optical access, metro access and metro backbone networks have been reviewed.

In terms of access networks, four simple protection measures as suggested in G.983.1 have been gone through. Those variations are simple but lack flexibility. Then two protection schemes with star-ring-bus and group protection architecture were reviewed. It inspires the insight that access network service can be more flexible with better protection capability.

In terms of metro access and metro backbone networks, various self-healing ring architectures have been reviewed. Previous protection schemes for virtual star and virtual mesh topology have been discussed.

In the following chapters, novel self-healing architectures for multiwavelength optical access, metro access and metro backbone networks will be proposed respectively in chapter 3, 4 and 5.

Chapter 3
Self-Healing Network Architecture for WDM Optical Access Networks

3.1 Introduction

The primary communication channels to most residents are the twisted pair of telephone network and the coaxial cable of CATV network. These service networks are essentially complementary in both bandwidth and delivery method: telephony is the epitome of a narrowband service that is switched, whereas CATV is the epitome of a broadband service that is broadcast. Unfortunately, there is a perceived need for future network to be both broadband and switched. This perceived need for bandwidth to the home tended to force fiber as the transmission medium. Time Division Multiplexing Passive Optical Network (TDM-PON) [22][23][24] has been proposed as a solution for broadband access networks. The using of passive cable plant in RN greatly reduced the initial cost and maintenance cost of the access networks.

In the past decade, as the explosive growth of Internet traffic and the convergence of telecommunication, Internet and broadcast networks services are causing huge demand on bandwidth. Broadband networking technologies such as wavelength-division-multiplexed passive optical networks (WDM-PONs) [25][26] have been emerging as the most popular systems in the access network architecture and have been extensively studied throughout the past decade for last mile applications. It enhances the penetration of WDM technology further towards the subscriber side, enabling the delivery of services with higher capacity to the subscribers. Thus, reliable access network architectures are highly desirable. However, little work has been done to offer the protection capability in the optical access networks.

In this chapter, we will propose two novel self-healing network architectures for WDM-PONs which can provide full path protection capability against any fiber-cut between the remote node (RN) and the optical network units (ONUs), as well as that between the RN and the optical line terminal (OLT).

3.2 Star-Ring Protection Architecture (SRPA)

3.2.1 Motivation

The previously proposed group protection architecture (GPA) for WDM-PON networks [15][16] can only provide protection against fiber link failure between the RN and the ONUs. However, the bi-directional traffic cannot be restored under the fiber link failure between the OLT and the RN.

In this section, we propose and investigate a new self-healing network architecture for

WDM PON access network, called star-ring protection architecture (SRPA), so as to integrate and extend the capability to protect against fiber link failure between the RN and the ONUs, as well as that between the RN and the OLT. The bi-directional traffic under single or multiple link failures could be promptly restored.

3.2.2 Network topology of SRPA

Fig. 3.1 shows our proposed star-ring protection architecture for WDM-PONs. At the OLT, the downstream signals are multiplexed through a $1\times N$ AWG, duplicated by a coupler and transmitted to the RN on feeder fibers F_1 and F_2, respectively. At the RN, the fibers F_1 and F_2 are connected to the input ports 1 and 2 of a $2\times N$ AWG, respectively, and these AWG input ports correspond to two adjacent passband channels. The value of N is chosen to be an even number. And ONU(i) (for i=1,..N) is connected to the ith output port of the AWG at the RN by a piece of optical fiber, denoted as L_i. A piece of protection fiber, denoted as $P_{i,(i+1)}$, is connected between the ONU(i) and the ONU(i+1), except that the $P_{N,1}$ will be connecting ONU(N) and ONU(1) to close the ring. The resultant network topology can be visualized as a three-dimensional star-ring structure, as shown in the Fig. 3.1.

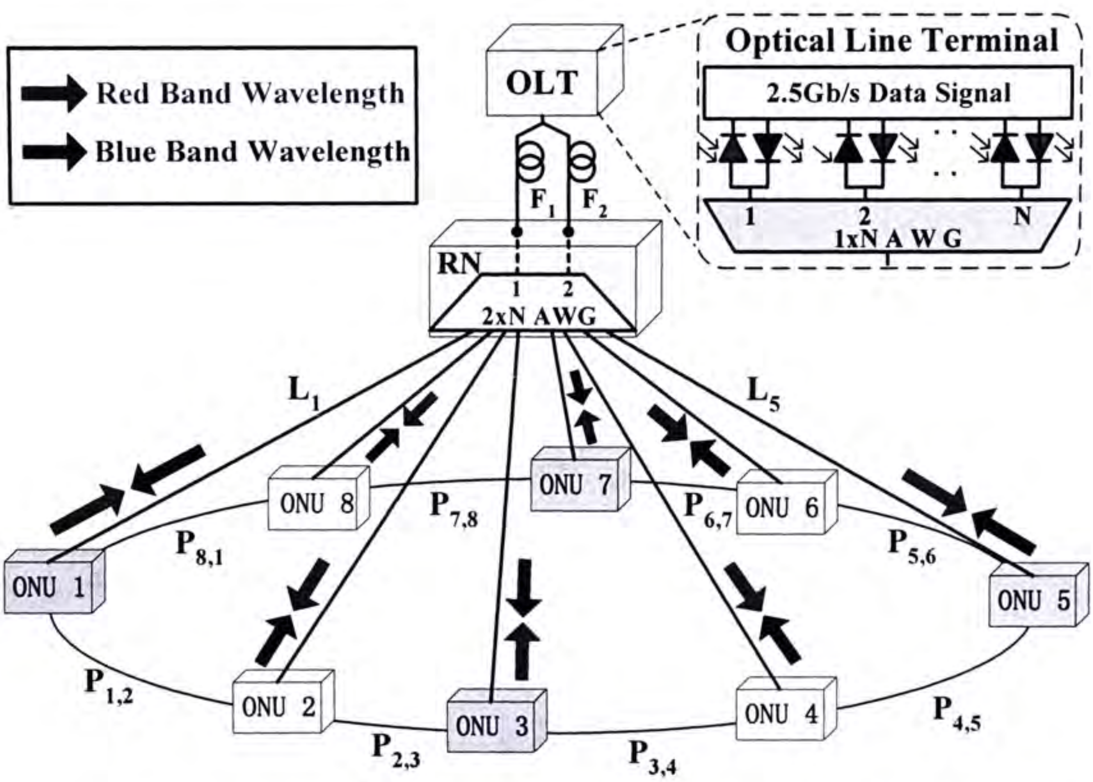

Fig. 3.1 Proposed Star-Ring Protection Architecture for WDM-PON with eight ONUs;

3.2.3 Wavelength assignment of SRPA

Fig. 3.2 illustrates the wavelength assignment plan, based on ITU wavelength grid.

The downstream and the upstream wavelength channels are interleaved with each other for the ONUs. For each ONU, the up- and downstream wavelengths, of which one is in blue band while the other is in red band, are separated from each other by one free-spectral range (FSR) of the AWG. ONUs with odd indices are assigned with their respective downstream wavelengths in blue band and upstream wavelengths in red band, whereas ONUs with even indices are assigned with their respective downstream wavelengths in red band and upstream wavelengths in blue band, as illustrated in the table of Fig. 3.2.

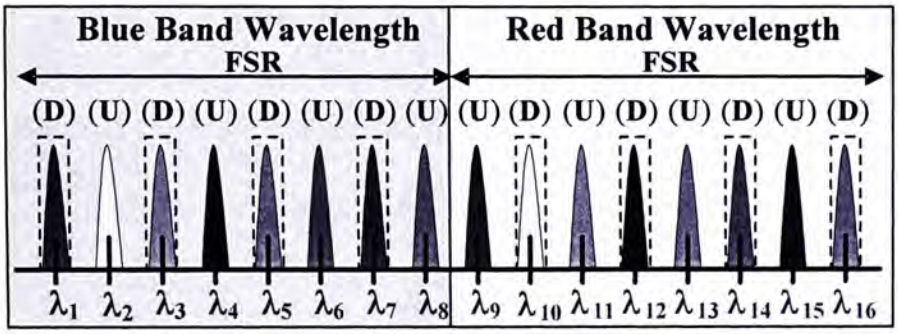

ONU	1	2	3	4	5	6	7	8
D	λ_1	λ_{10}	λ_3	λ_{12}	λ_5	λ_{14}	λ_7	λ_{16}
U	λ_9	λ_2	λ_{11}	λ_4	λ_{13}	λ_6	λ_{15}	λ_8

*Note: D - Downstream wavelength; U - Upstream wavelength

*The downstream wavelength for each ONU is marked with the dot box.

Fig. 3.2 Wavelength assignment plan for N=8. Note λ_i, (for i=1,..,16) are the wavelength grid indices, and FSR stands for free-spectral range of the 2×N AWG.

3.2.4 Structure of ONU

Fig. 3.3 illustrates the structure of ONUs under normal operation. The downstream wavelengths λ_i (for i is odd) and λ_{i+N} (for i is even), destined for the ONU(i)s are carried via the feeder fiber F_1, the AWG at the RN and the distribution fiber L_i. Due to the presence of the additional fiber feeder F_2 and the channel-shifting input-output property of the AWG, each downstream wavelength (denoted with brackets in Fig. 3.3) is also delivered to its respective adjacent ONU(i-1). Thus, with the wrap-around spectral periodicity property of the AWG, at any particular ONU(k) (for i=1,..N), two downstream wavelengths, {λ_k, λ_{k+N+1}; for k is odd} or {λ_{k+N}, λ_{k+1}; for k is even}, will be received. The former wavelength is designated for ONU(k) in normal operation; while the latter one is a duplicated copy of the downstream wavelength destined for ONU(k+1) and this serves for protecting ONU(k+1) via ONU(k). On the other hand, ONU(k) supports its upstream wavelength {λ_{k+N}; for k is odd} or {λ_k ; for k is even} in normal operation. However, in protection mode, the ONU(k) can also simultaneously support {λ_{k+1}; for k is odd} or {λ_{k+N+1}; for k is even}, which is routed from ONU(k+1), in addition to its own designated upstream wavelength.

The adjacent ONUs are connected by a piece of protection fiber in a ring form. At the front-end of each ONU, an optical coupler is used to duplicate the downstream signals, of which one set is destined to itself and the other set is routed to its adjacent connected ONU for protection purpose. A 1x2 optical switch is incorporated in each ONU to select the wavelength signals from the appropriate side. Under normal operation, the switch is configured to the upper port and selects the downstream signals from the RN. A Red/Blue (R/B) filter is further used to separate the upstream and the downstream wavelength channels; and also route the protection downstream wavelength towards the laser transmitter (LD) where it will be blocked by the internal isolator of the LD.

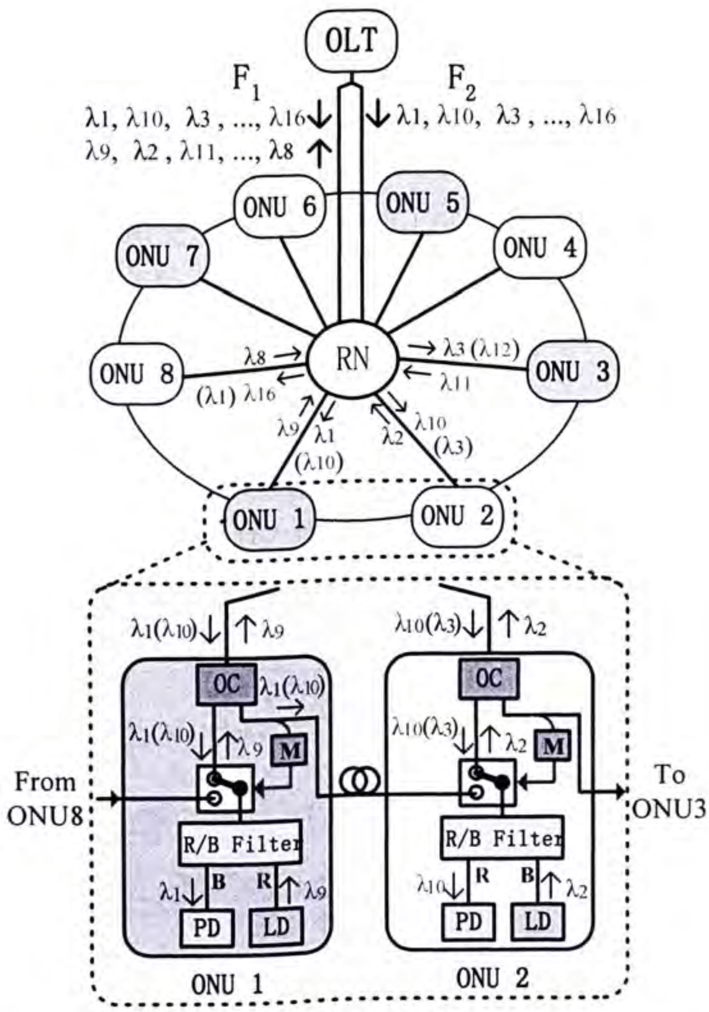

Fig. 3.3 ONU configuration under normal operation. OC: optical coupler; M: monitoring unit.

3.2.5 Protection mechanism

There are two types of fiber failures: Type I (link failure(s) between ONU and RN) and Type II (feeder fiber failure between OLT and RN). Fig. 3.4 illustrates the ONUs configuration under single Type I failure between the RN and ONU(2), for instance. A drastic drop in power at the monitoring unit (M) of ONU(2) will be detected. Thus, the optical switch inside ONU(2) will be automatically reconfigured to the lower port, as illustrated in Fig. 3.4. Both the upstream and the downstream wavelengths of the isolated ONU(2) will be routed to/from the ONU(1) via the protection fiber between them. Thus, with the channel-shifting property of the AWG at the RN, they can still be routed to the OLT via the feeder fiber F_2, as shown in Fig. 3.4. With this protection mechanism, a fast restoration of fiber failure can be achieved, without any disturbance on the existing traffic and other ONUs.

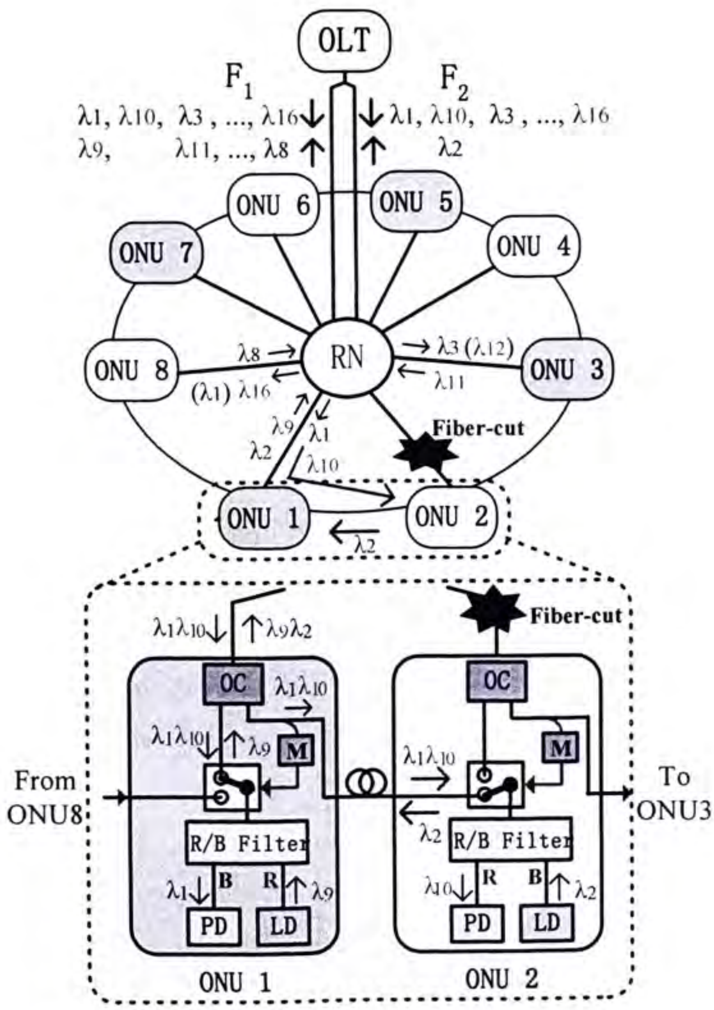

Fig. 3.4 ONU configuration under single Type I failure. OC: optical coupler; M: monitoring unit.

If there exists multiple Type I link failures, the SRPA can still be able to protect and restore the affected traffic using the above mentioned mechanism, provided that such multiple Type I link failures do not occur at two adjacent ONUs simultaneously, as illustrated in Fig. 3.5(a). On the other hand, for Type II fiber feeder failure, for example, the fiber feeder F_1 is broken between the RN and the OLT, the protection mechanism is similar to that in Type I except that the monitoring units in all ONUs will trigger the respective optical switches, simultaneously. The wavelength channels for each ONU will be routed via its adjacent ONU and all wavelengths from all the ONUs will be routed back to the OLT via the fiber feeder F_2, as illustrated in Fig. 3.5 (b).

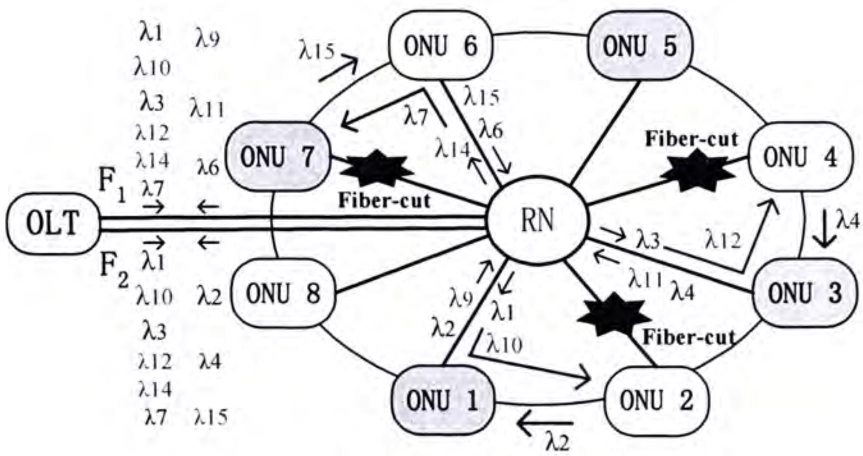

(a)

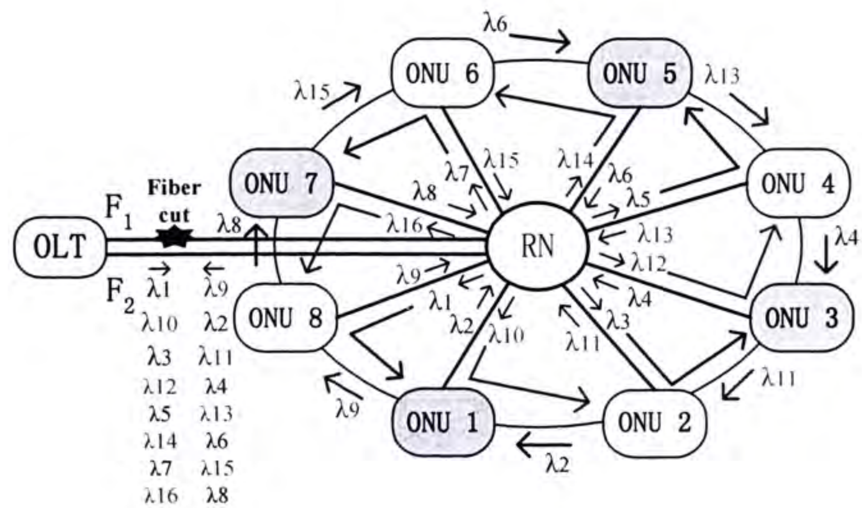

(b)

Fig. 3.5 (a) Multiple Type I failure protection; (b) Type II feeder fiber, F_1, failure protection.

3.2.6 Experimental demonstration

The transmission performance and the protection switching of our proposed network were experimentally investigated, using the setup similar to Fig. 3.3. Two ONUs have been implemented to demonstrate the operation principle. 2.5-Gb/s directly modulated

DFB laser diodes were used at the OLT and the ONUs. A 16×16 AWG, with 100-GHz channel spacing and a free-spectral range (FSR) of 12.8nm, was used at the RN. It was also connected to the 1×16 AWG, as the channel multiplexer, at the OLT via a pair of 22-km standard single-mode fibers (SMF), as the fiber feeders. The Red/Blue filters used at the ONUs had 18-nm passband at both red and blue bands. A piece of 4-km protection fiber was used to connect the two ONUs. Each ONU was incorporated with one 1×2 opto-mechanical optical switch to re-route the wavelength under the protection mode. Under this configuration, the optical power of the downstream and upstream signals from the OLT to the ONU(2) was monitored. Both single Type I and Type II fiber link failures were simulated by intentionally disconnect the fiber connections. The bit-error-rate (BER) performance under both the normal and the protection path were measured and was depicted in Fig. 3.6. In all cases, the measured receiver sensitivities at BER=10^{-9} were very close to each other. The small induced power penalty (<0.5dB) compared to the back-to-back measurement was due to chromatic dispersion of the directly modulated wavelength channels.

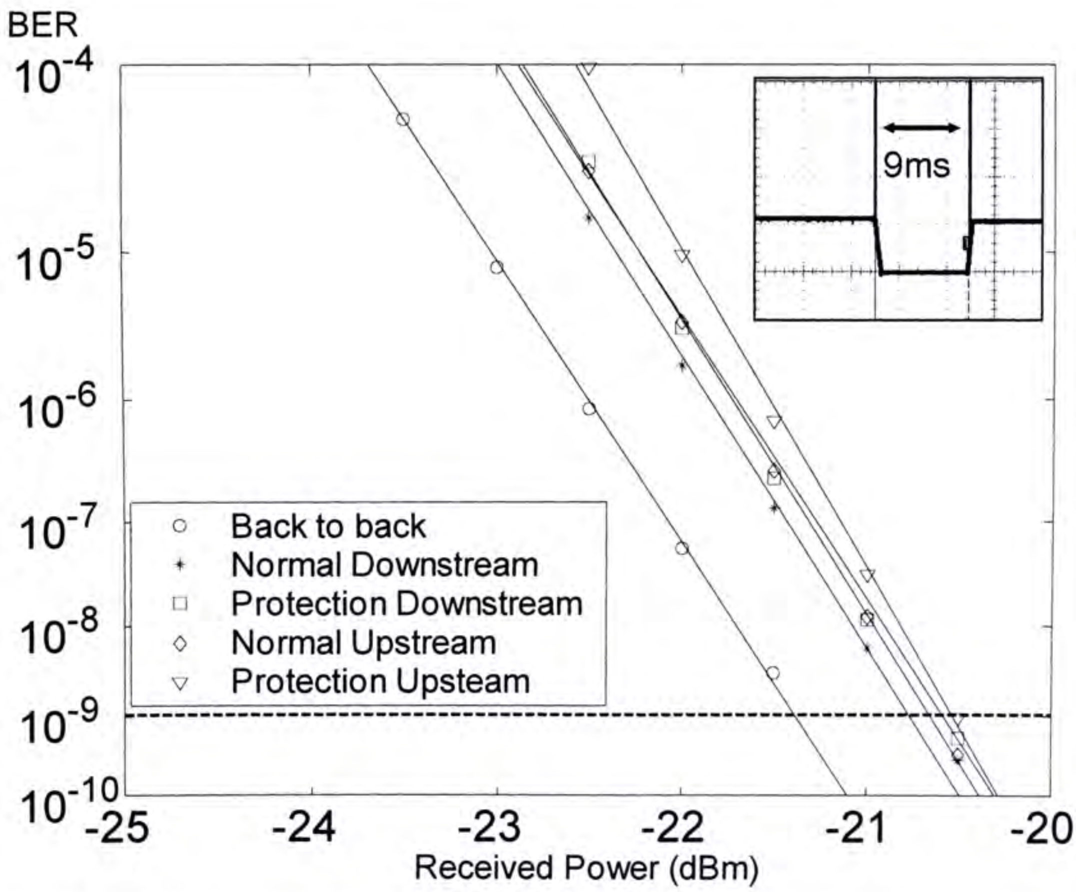

Fig. 3.6 BER measurement under both normal and the protection modes. Inset shows the switching time measurement under the protection mode.

The switching time or the restoration time in case of the simulated fiber cut was also monitored. The result was shown in the inset of Fig. 3.6. The waveform showed the signal measured at the monitoring unit in ONU(2). The switching time was measured to be about 9 ms which is mainly determined by the switching performance of the opto-mechanical switches we used, while the decision time of monitoring circuit and the propagation time are relatively negligible. This 9-ms switching time corresponded to the network traffic restoration time achieved.

3.2.7 Power budget

Assuming the transmitted powers from the LDs in the ONUs are 0dBm, the receiver sensitivities of the photodiodes at the OLT are -20dBm (at 2.5-Gb/s), the insertion losses of optical switches, AWG and Red/Blue filters are 1dB, 5dB and 1dB, respectively; the optical power margin will be 10dB in the re-routing path of upstream traffic and so is that in downstream traffic. Therefore, a transmission distance of more than 40 km can be achieved.

3.2.8 Summary

We have proposed a novel star-ring protection architecture (SRPA) for WDM-PONs. By incorporating simple optical switches and filters into the ONUs, and by connecting ONUs in the proposed star-ring structure, full protection capability can be achieved. Thus the isolated ONUs can still communicate with the OLT in case of any fiber cut in the PON with minimum disturbance to its neighborhood. Compared to the network architecture in [15], the proposed star-ring network architecture can protect against both fiber link failure between the RN and the ONUs and that between the RN and the OLT simultaneously. Furthermore, we employed a novel wavelength assignment scheme to reduce the amount of required network resources.

3.3 Duplicated-Tree Protection Architecture (DTPA)

3.3.1 Motivation

In order to further increase the survivability of WDM-PON, in this section, by duplicating the AWG in the RN, we propose and investigate a Duplicated-Tree Protection Architecture (DTPA) for WDM PON with simple ONUs. By using the spectral periodicity of the AWG, a novel wavelength assignment plan is proposed and a simple alternate-path switching scheme is employed for protection against both feeder and distribution fiber link failures, as well as the AWG failure at the RN simultaneously. The design and the protection strategies under various failure scenarios will be discussed.

3.3.2 Network topology and wavelength assignment

Fig. 3.7(a) shows our proposed WDM PON architecture with N ONUs, where $N = 8$, for example. At the OLT, the downstream signals are multiplexed through an $N\times2$ AWG and routed either to the AWG_1 in the RN through feeder fiber F_1 or to the AWG_2 through feeder fiber F_2. The ONUs with odd indices are connected to the first $N/2$ output ports of the AWG_1 and the AWG_2 via 2×2 couplers; while those with even indices are connected to the last N/2 output ports of the AWG_1 and the AWG_2, as shown in Fig. 3.7(a). Fig. 3.7(b) illustrates the proposed wavelength assignment plan. For index i=1,...,(N/2), the wavebands A (λ_i) and B ($\lambda_{N/2+i}$) in the blue band are allocated for the downstream and the upstream wavelength channels of the ONUs with odd indices (ONU_{2i-1}), respectively, while the wavebands C (λ_{N+i}) and D ($\lambda_{3N/2+i}$) in the red band are for the downstream and the upstream wavelength channels of the ONUs with even indices (ONU_{2i}), respectively. Besides, the free-spectral range (FSR_2) of AWG_1 and AWG_2 at the RN is half of the FSR_1 of the AWG at the OLT. The wavelength λ_i is separated from λ_{N+i} by one FSR_1 of the AWG at the OLT; while the downstream and the upstream wavelengths assigned to each ONU are separated by half of the FSR_1. Under normal operation, each downstream wavelength originated from the OLT is destined for its respective ONUs through either the AWG_1 or AWG_2 at the RN. In contrast, the upstream wavelengths are duplicated by 2×2 couplers in each ONU and traverse towards the OLT through both AWGs at the RN, as illustrated in Fig. 3.7(a).

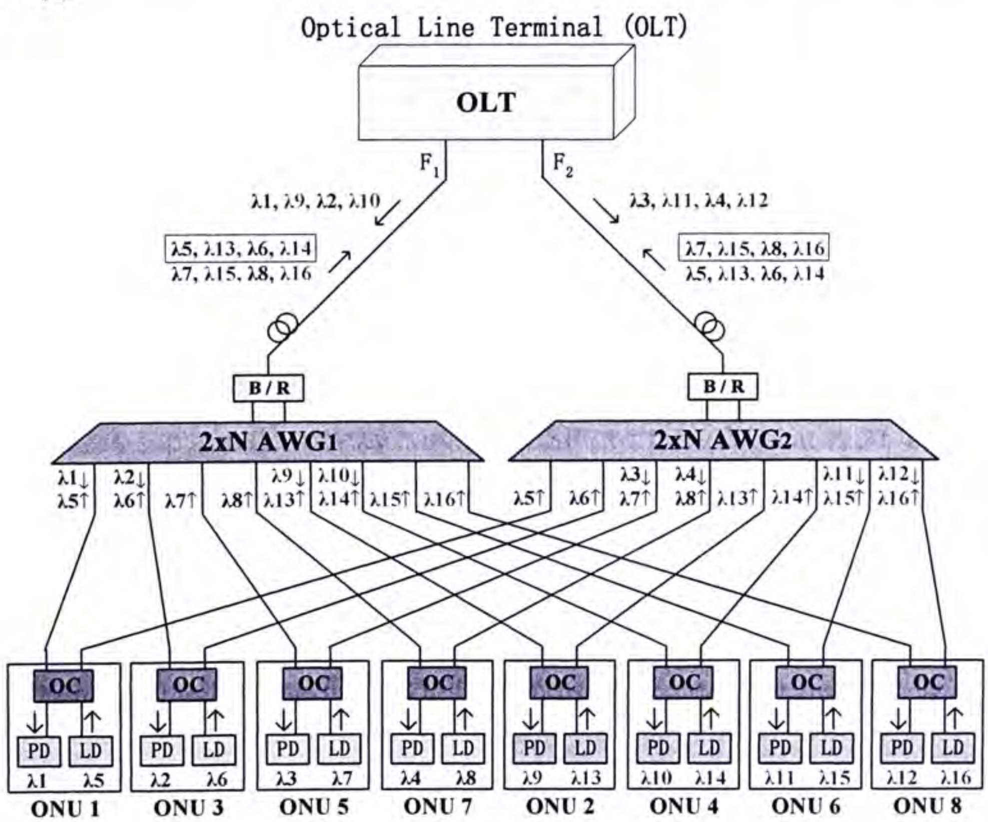

(a)

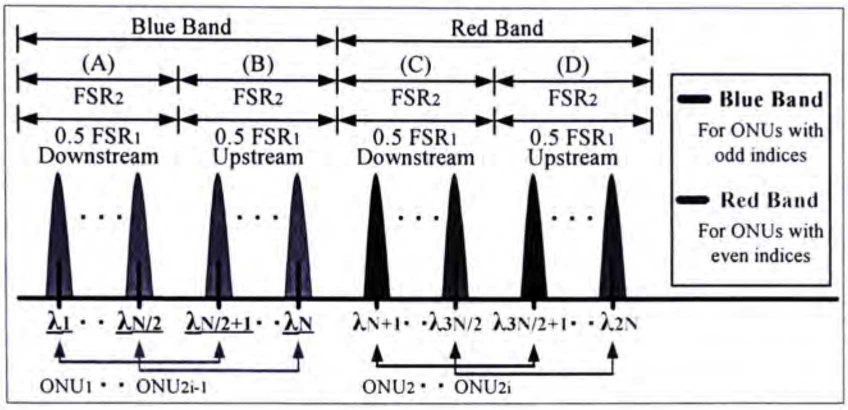

(b)

Fig. 3.7 (a) Proposed WDM-PON Architecture with eight ONUs; (b) wavelength assignment plan. B/R: Blue Red filter; OC: optical coupler. Note FSR_1 stands for free-spectral range of the N×2 AWG at the OLT; while FSR_2 stands for that of both AWG_1 and AWG_2 at the RN. The wavelengths quoted in boxes are the working upstream wavelengths.

3.3.3 Structure of OLT

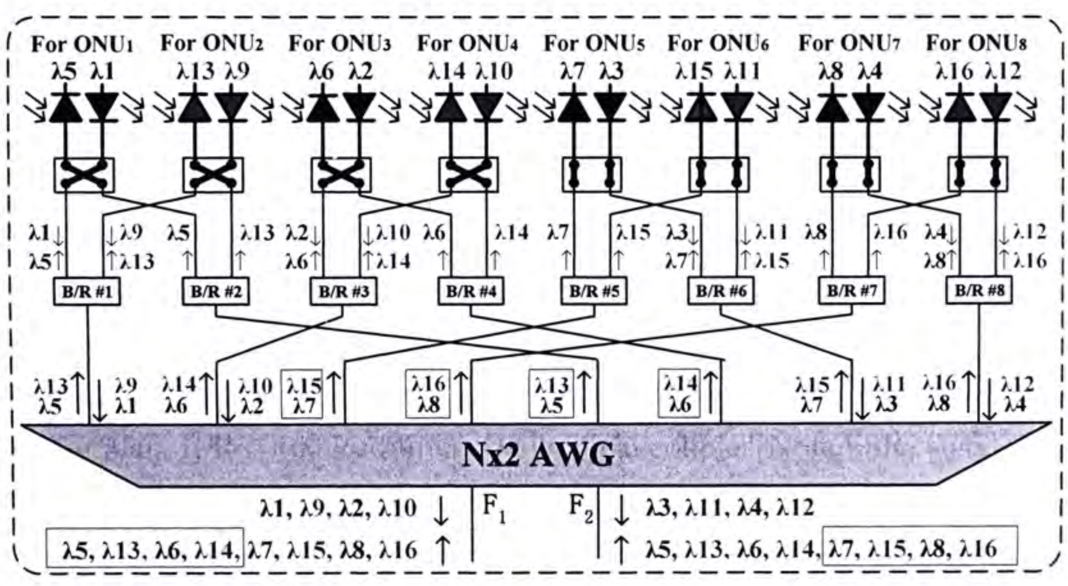

Fig. 3.8 OLT configuration under normal operation

As shown in Fig. 3.8, the OLT consists of an N×2 (N=2n) AWG and M ($M \leqq N$) transceivers. Each transceiver, designated for a particular ONU, is associated with a 2×2 optical switch and a Blue/Red filter. Every two adjacent transceivers form a group and communicate with their respective ONUs, one with odd index (2i-1) and the other with even index (2i), respectively. Under normal operation, the 2×2 optical switches associated with ONU_1, ONU_2, …, $ONU_{N/2}$ are in cross states; while those associated with $ONU_{N/2+1}$, $ONU_{N/2+2}$, …, ONU_N are in bar states to balance the traffic on the AWG_1 and the AWG_2 at the RN. For ONU_{2i-1} (say ONU_1), the transmitter with downstream wavelength λ_i (say λ_1) and the receiver with upstream wavelength $\lambda_{N/2+i}$ (say λ_5), both of which are in the blue band, are connected to the respective blue-band ports of the two Blue/Red filters (say B/R#1 and B/R#2) in the same group, respectively, as depicted in Fig. 3.8 and Fig. 3.7(b). Similarly, for ONU_{2i} (say ONU_2), the transmitter with downstream wavelength λ_{N+i} (say λ_9) and the receiver with upstream wavelength $\lambda_{3N/2+i}$ (say λ_{13}), both of which are in the red band, are connected to the respective red-band ports of the two Blue/Red filters (say B/R#1 and B/R#2) in the same group, respectively. In general, the combined port of the B/R#(2i-1) (say B/R#1) and that of the B/R#(2i) (say B/R#2) are connected to the i^{th} (say 1^{st}) and the $(N/2+i)^{th}$ (say 5^{rd}) input ports of the N×2 (say 8×2) AWG, respectively. The spectral transmission peaks of the two output ports of the AWG are spaced by half of its FSR_1, and each of them are connected to the either feeder fiber F_1 or F_2. The downstream wavelengths for the first $N/2$ ONUs will be propagating through AWG_1; while those for the last $N/2$ ONUs will be propagating through AWG_2 at the RN, respectively. At the RN, each of the feeder fibers F_1 and F_2 are connected to a Blue/Red filter, which is connected to input ports of 2×N AWG_1 and AWG_2, respectively. The spectral transmission peaks of those ports are spaced by half of its FSR_2. Thus, the wavelengths in blue band will be transmitted to the first $N/2$ output ports; while those in red band will be transmitted to the last $N/2$ output ports. Since the FSR_2 of the AWGs in the RN is half of the FSR_1 of the AWG at the OLT, the downstream and the upstream wavelengths for each ONU will be transmitted through the same output port of the AWGs at the RN. At each ONU, the upstream will be sent out via both AWG_1 and AWG_2, thus two copies of the upstream wavelengths originating from all ONUs will reach the N×2 AWG, where they are demultiplexed and routed towards the transceivers at the OLT, via the respective Blue/Red filters and 2×2 optical switches. One of the copies of the upstream wavelengths traverses through the path which the corresponding downstream wavelength passes would reach their respective upstream receivers; while the other copy of the upstream wavelengths would reach the transmitters where they would be blocked by the built-in optical isolators of all transmitters at the OLT. Fig. 3.7(a) and Fig. 3.7(b) illustrate the flow of the downstream and the upstream wavelengths under normal operation.

3.3.4 Protection mechanism

In case of any fiber cut, the OLT will detect the loss of some upstream signals. Such conditions will trigger all the 2×2 optical switches associated with the transceivers designated for the affected ONUs at the OLT to toggle their switching states automatically. As a result, all the blocked downstream wavelengths can be routed to the affected ONUs through the other AWG at the RN along the other available path;

while all the respective upstream receivers at the OLT can still receive a copy of the upstream wavelengths. Fig. 3.9(a) illustrates the flow of the downstream and the upstream wavelengths when the fiber between RN and ONU_1 is broken, as an example. Under this condition, the downstream wavelength for ONU_1 (λ_1) could not reach ONU_1 via the AWG_1. Thus the protection switching at the OLT re-routes λ_1 to go along the AWG_2 and reach the downstream receiver at ONU_1. At the same time, the upstream wavelength λ_5 from ONU_1 would reach the respective upstream receiver at the OLT via a different path, as illustrated in Fig. 3.9(a). In the same way, feeder fiber failure and AWG failure at the RN can be also protected. Traffic can be restored under multiple failures provided that at least one path is available between the OLT and each ONU, either through AWG_1 or AWG_2, as illustrated in Fig. 3.9(b). With this proposed protection mechanism, a fast restoration of fiber failures and AWG failure at the RN can be achieved and all protection switching operations are performed at the OLT only.

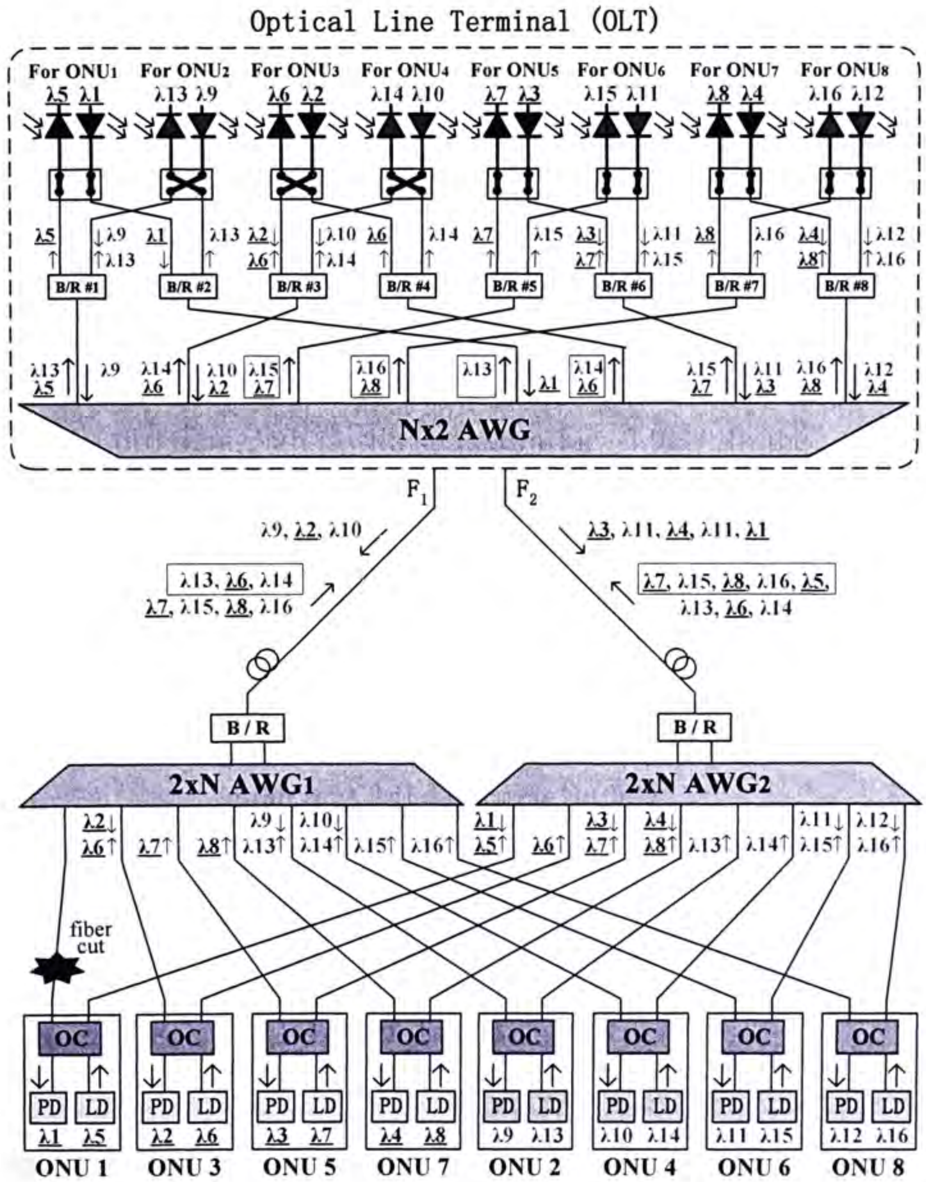

(a)

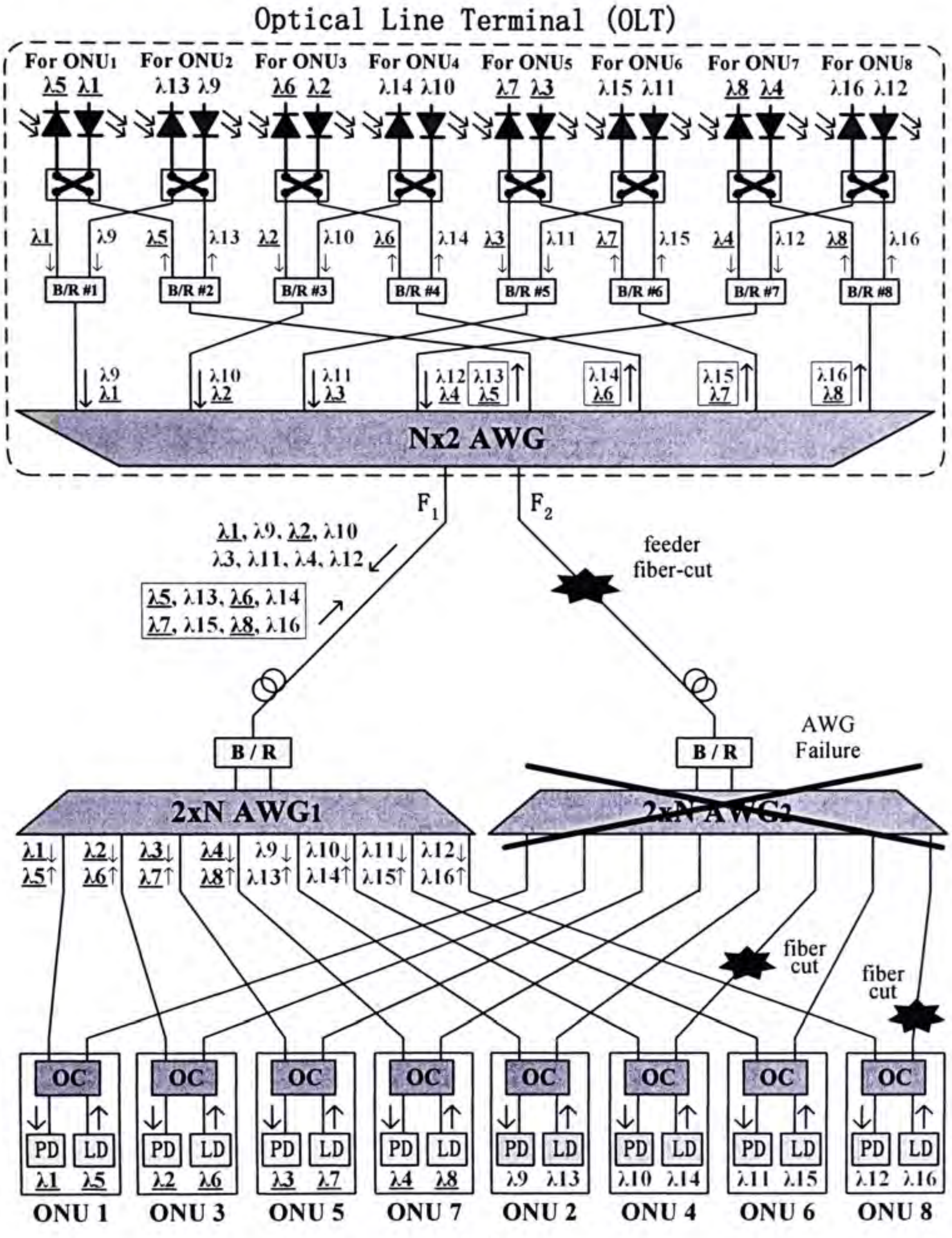

(b)

Fig. 3.9 OLT configuration under (a) distribution fiber link failure; (b) multiple failures. B/R: Blue Red filter; OC: optical coupler.

3.3.5 Experimental demonstration

The transmission performance and the protection switching of our proposed network were experimentally investigated, using the setup similar to Fig. 3.7. ONU_1 has been implemented to demonstrate the operation principle. 2.5-Gb/s directly modulated DFB laser diodes were used at the OLT and ONUs. A 16×16 AWG, with 100-GHz channel spacing and a FSR_1 of 12.8nm, was used at the OLT. It was also connected to two 1×16 AWGs, with 50-GHz channel spacing and a FSR_2 of 6.4nm, at the RN via a pair of 22-km standard single-mode fibers (SMF), as the feeder fibers. The optical spectrums of the AWGs in the OLT and RN were shown in the Fig. 3.10(a). The Blue/Red filters used at the OLT and RN had 18-nm passband at both red and blue bands. Each transceiver at the OLT was incorporated with one 2×2 optical switch to re-route the wavelength under the protection mode. Under this configuration, the optical power of the upstream signals from the ONU_1 to the OLT was monitored. Fiber link failures were simulated by disconnect the fiber connections. The bit-error-rate (BER) performance under both the normal and the protection path were measured and was depicted in Fig. 3.10(b). In all cases, the measured receiver sensitivities at BER=10^{-9} were very close to each other. The small induced power penalty (< 0.5dB) compared to the back-to-back measurement was due to chromatic dispersion of the directly modulated wavelength channels.

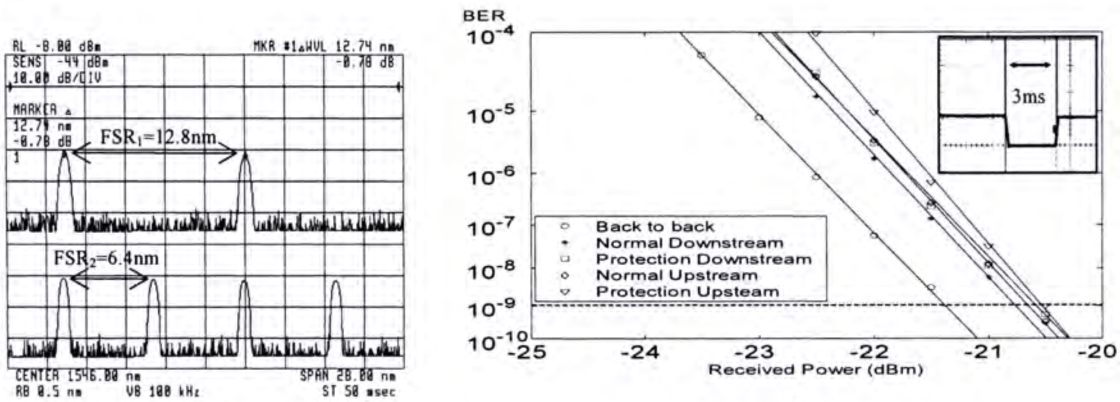

(a) (b)

Fig. 3.10 (a) The optical spectra of the AWGs at the OLT (upper) and RN (lower); (b) BER measurement of the downstream wavelengths for both the normal and the protection modes. Inset shows the switching time measurement under the protection mode.

The switching time or the restoration time in case of the simulated fiber cut was also monitored. The result was shown in the inset of Fig. 3.10(b). The waveform showed the signal measured at the monitoring unit in OLT. The switching time was measured to be about 3 ms and this corresponded to the network traffic restoration time achieved.

1.1.1 Summary

We have proposed and investigated a Duplicated-Tree Protection Architecture for WDM-PON. By incorporating simple optical switches and filters into the OLT, and by duplicating the AWG in the RN, full protection against feeder and distribution fiber link failures as well as the AWG failure in the RN can be achieved simultaneously. With the proposed alternate-path switching scheme, the protection switching is performed at the OLT only.

1.4 Summary

In this chapter, we propose two self-healing network architectures for WDM-PON optical access networks. The first one (Star-Ring Protection Architecture) can provides protection against link failure between the RN and the ONUs, as well as that between the RN and the OLT; while the second one (Duplicated-Tree Protection Architecture) further extends the capability to protect against the AWG failure in the RN simultaneously, so that the network survivability is highly increased.

Chapter 4
Single-Fiber Self-Healing WDM Ring Network Architecture for Metro Access Networks

4.1 Introduction

Network survivability is necessary for high-speed optical fiber networks. The ring topology has been considered as a cost-effective survivable network architecture due to bandwidth sharing and improved survivability [27]. Bidirectional wavelength-division-multiplexing (WDM) self-healing ring (SHR) network with full mesh traffic connection pattern has been demonstrated for metro backbone networks [28] to save optical fibers and optical components. These architectures are based on bidirectional add–drop multiplexers (BADMs) that are configured to support full mesh connectivity between the nodes in the ring networks. However, in metro access networks, traffic from many access nodes (ANs) is transmitted/received to/from a hub node, and the hub node controls the traffic between ANs [29]. Since this class of network connects the metro backbone networks and access networks, self-healing network architectures are desired to assure reliable data delivery and a simple low cost add–drop multiplexer is required to connect the hub node and ANs.

In this chapter, in order to further reduce the cost and simplify the access node, we propose and demonstrate a new single-fiber bi-directional WDM SHR metro-access ring network, comprising a hub node and multiple access nodes (ANs). Each AN is incorporated with a simple low-cost B-OADM for adding/dropping wavelength channels to/from the hub node. By making use of the spectral periodicity of the $N\times2$ array waveguide grating (AWG) at the hub node, a novel wavelength assignment plan is proposed to facilitate both the bi-directional data transmission as well as the proposed alternate-path switching scheme for protection against any single fiber failure in the network. The proposed ring network can realize traffic restoration without the need of an extra protection fiber nor doubling the number of optical transceivers.

4.2 Network architecture and wavelength assignment

Fig. 4.1 shows our proposed single-fiber bi-directional metro-access network with one hub node and N ANs. Each node is equipped with one pair of downstream receiver and upstream transmitter while the hub node has N pairs of downstream transmitters and upstream receivers. Therefore, altogether $2N$ wavelengths are required. All data traffic collected from all ANs is terminated and routed through the hub node.

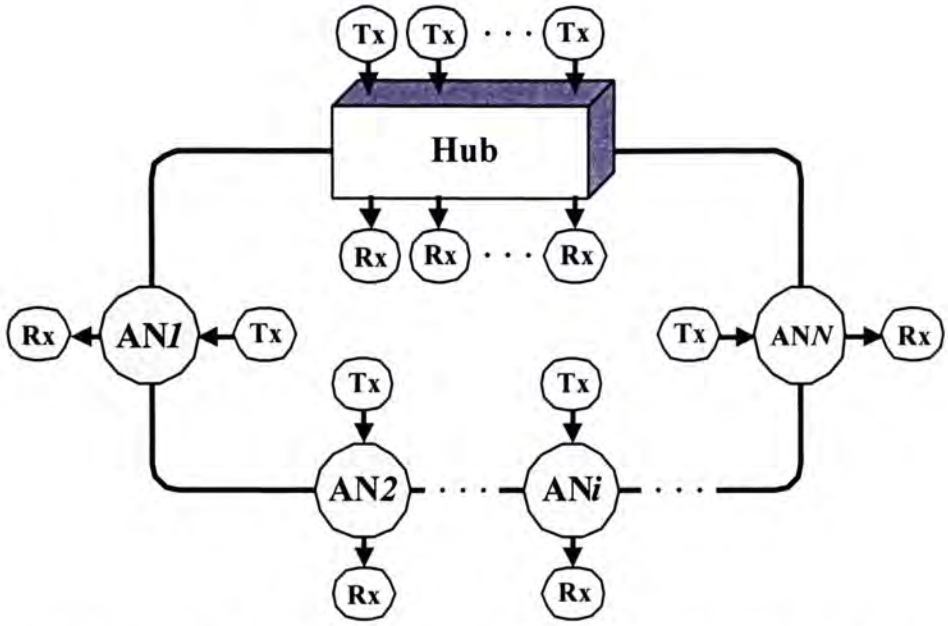

Fig. 4.1 Single-fiber bidirectional metro-access ring with N ANs.

Fig. 4.1 illustrates the proposed wavelength assignment plan. For index i=1,...,(N/2), the wavebands A (λ_i) and B ($\lambda_{N/2+i}$) in the blue band are allocated for the downstream and the upstream wavelength channels of the ANs with odd indices (AN_{2i-1}), respectively, while the wavebands C (λ_{N+i}) and D ($\lambda_{3N/2+i}$) in the red band are for the downstream and the upstream wavelength channels of the ANs with even indices (AN_{2i}), respectively. Besides, wavelength λ_i is separated from λ_{N+i} by one free-spectral range (FSR) of the AWG at the hub node; while the upstream and the downstream wavelengths assigned to each AN are separated by half of the FSR. Equivalently, for k=1,...,N, ANk is assigned with $\lambda_{(k+1)/2}$ and $\lambda_{(N+k+1)/2}$ as the downstream and the upstream wavelengths, respectively, for odd k, while ANk is assigned with $\lambda_{(2N+k)/2}$ and $\lambda_{(3N+k)/2}$ as the downstream and the upstream wavelengths, respectively, for even k. For instance, for a 4-node (N=4) network with eight wavelength channels (λ_1 to λ_8), the designated (downstream(D), upstream(U)) wavelength pair for AN1, AN2, AN3 and AN4 are (D=λ_1, U=λ_3), (D=λ_5, U=λ_7), (D=λ_2, U=λ_4), and (D=λ_6, U=λ_8), respectively (see Fig. 4(a)). Note that λ_1, is one FSR way from λ_5; and so are the wavelength pairs (λ_2, λ_6), (λ_3, λ_7), and (λ_4, λ_8). Besides, λ_1 is half of an FSR way from λ_3; and so are so are the wavelength pairs (λ_2, λ_4), (λ_5, λ_7), and (λ_6, λ_8). Under normal operation, each of the downstream wavelengths originated from the hub node is destined for its respective ANs in either clockwise (CW) or counter-clockwise (CCW) direction, whichever having the shortest path. In contrast, each of the upstream wavelengths from each AN traverses towards the hub node in both CW and CCW directions.

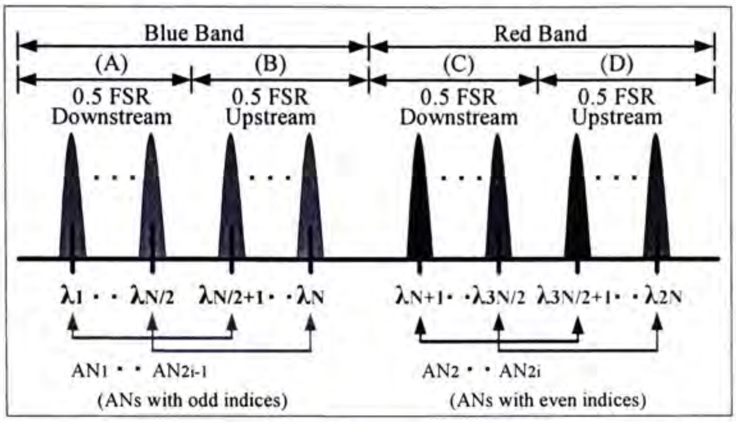

Fig. 4.2 Proposed wavelength assignment plan. FSR: free-spectral range of AWG; N: the number of wavelengths in one free-spectral range of AWG.

4.3 Structure of access node

The block diagram of the B-OADM at ANk is shown in Fig. 4.3. The upstream wavelength λ_u ($u=(N+k+1)/2$ for odd k or $u=(3N+k)/2$ for even k) is added and transmitted to the hub node in both CW and CCW directions; while the downstream wavelength λ_d ($d=(k+1)/2$ for odd k or $d=(2N+k)/2$ for even k) originating from either CW or CCW direction is dropped and transmitted to the receiver.

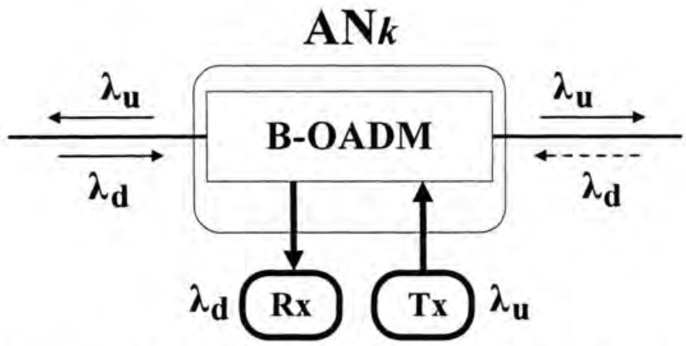

Fig. 4.3 Block diagram of the proposed B-OADM at AN_k. λ_u is the upstream wavelength ($u=(N+k+1)/2$ for odd k or $u=(3N+k)/2$ for even k); λ_d is the downstream wavelength ($d=(k+1)/2$ for odd k or $d=(2N+k)/2$ for even k). Note that λ_d reaches AN_k in either direction (solid or broken-line arrow) which has the shortest path from the hub only.

Fig. 4.4 and Fig. 4.5 show the two possible configurations of the B-OADM for AN_{2k-1} with odd indices for example. The first one (Fig. 4.4) is based on a Mach-Zehnder interferometer with identical fiber Bragg gratings on its arms (MZI-FBG) [31]. The upstream signal is added through the two optical couplers and transmitted to the hub node in both CW and CCW directions; while the downstream signal originating from either CW or CCW direction is dropped by the MZI-FBG and transmitted to the downstream receiver via an optical coupler. The MZI-FBG determines the dropped downstream wavelength, whereas the rest of other downstream wavelengths will simply bypass the AN. The second configuration (Fig. 4.5) is based on a four-port thin-film filter, which is used to simultaneously add and drop the upstream and the downstream wavelengths, respectively. Besides, other alternative B-OADMs could also be used as long as the add-drop functions described in the block diagram of Fig. 4.3 can be achieved.

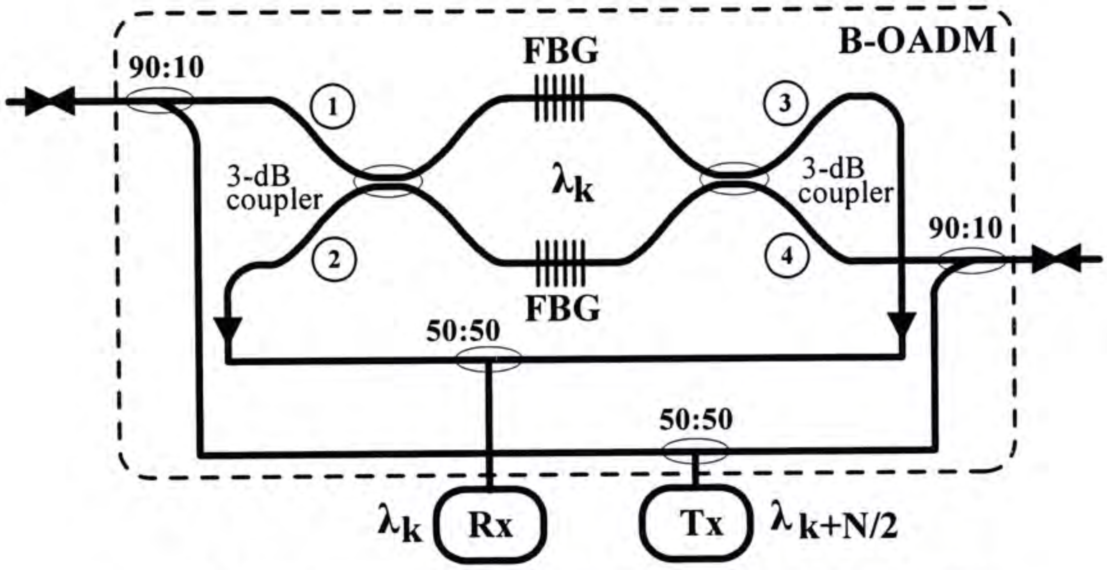

Fig. 4.4 Configuration of the MZI-FBG based B-OADM.

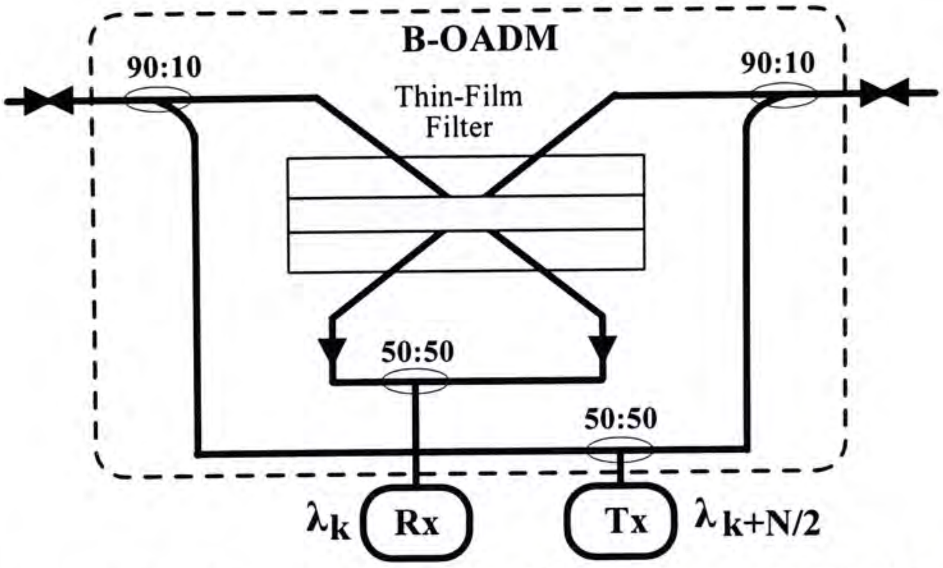

Fig. 4.5 Configuration of the thin-film filter based B-OADM .

4.4 Structure of hub node

Fig. 4.6 shows the network architecture and the hub node structure of the proposed single-fiber ring network with four nodes, i.e. N=4, for example, with eight wavelength channels (λ_1 to λ_8).

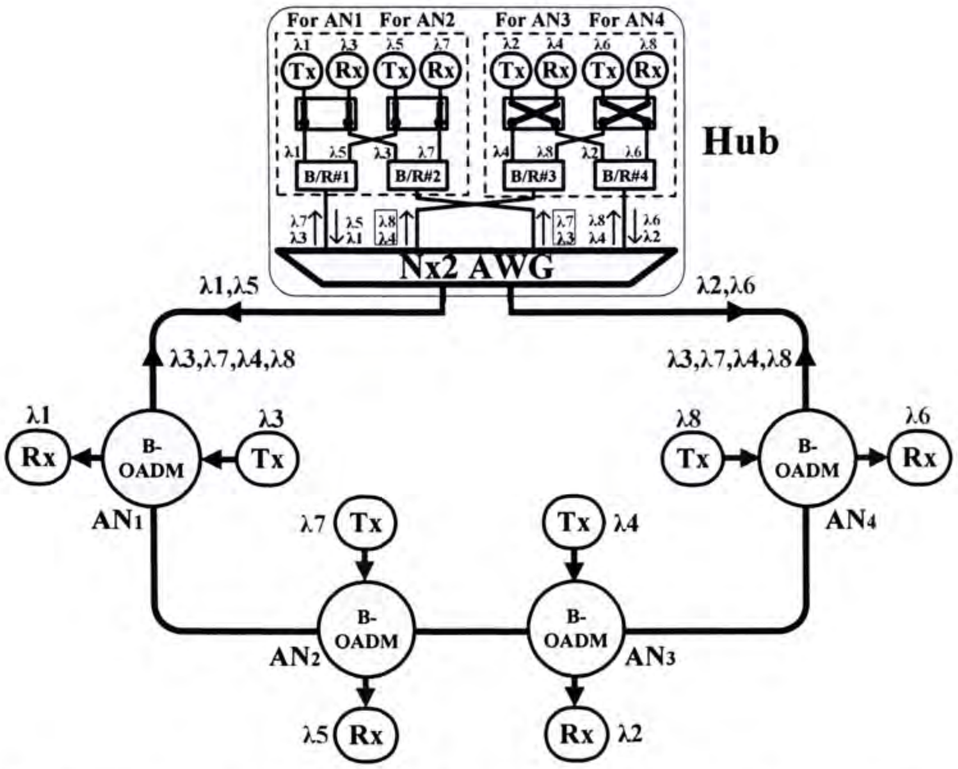

Fig. 4.6 Configuration of the proposed single-fiber bidirectional metro-access network under operation mode. B/R: Blue/Red band filter. Note: the wavelength channels marked with the boxes are the working upstream wavelength under operation mode.

The hub node consists of an $N\times2$ (N=2n) AWG and M ($M \leqq N$) transceivers. Each transceiver, designated for a particular AN, is associated with a 2×2 optical switch and a Blue/Red filter. Every two adjacent transceivers form a group and communicate with their respective ANs, one with odd index (2i-1) and the other with even index (2i), respectively. Under normal operation, the 2×2 optical switches associated with AN_1, AN_2, ..., $AN_{N/2}$ are in bar states while those associated with $AN_{N/2+1}$, $AN_{N/2+2}$, ..., AN_N are in cross states to choose the shortest path for the downstream signals. For AN_{2i-1} (say AN_1), the transmitter with downstream wavelength λ_i (say λ_1) and the receiver with upstream wavelength $\lambda_{N/2+i}$ (say λ_3), both of which are in the blue band, are connected to the respective blue-band ports of the two Blue/Red filters (say B/R#1 and B/R#2) in the same group, respectively, as depicted in Fig. 4.2 and Fig. 4.6. Similarly, for AN_{2i} (say AN_2), the transmitter with downstream wavelength λ_{N+i} (say λ_5) and the receiver with upstream wavelength $\lambda_{3N/2+i}$ (say λ_7), both of which are in the red band, are connected to the respective red-band ports of the two Blue/Red filters (say B/R#1 and B/R#2) in the same group, respectively. In general, the combined port of the B/R#(2i-1) (say B/R#1) and that of the B/R#(2i) (say B/R#2) are connected to the ith (say 1st) and the $(N/2+i)^{th}$ (say 3rd) input ports of the $N\times2$ (say 4×2) AWG, respectively. The spectral transmission peaks of the two output ports of the AWG are spaced by half of its FSR, and each of them are connected to the transmission fiber of the ring network in either CW or CCW direction. The downstream wavelengths with odd indices (say λ_1, λ_5) and even indices (say λ_2, λ_6) will be propagating in CCW and CW directions in the ring network, respectively. On the other hand, as each AN will send out its upstream wavelength in both directions, thus two copies of the upstream wavelengths (say λ_3, λ_4, λ_7, λ_8) originating from all ANs will reach the N×2 AWG, where they are demultiplexed and routed towards the transceivers at the hub, via the respective Blue/Red filters and 2×2 optical switches. One of the copies of the upstream wavelengths would reach their respective upstream receivers; while the other copy of the upstream wavelengths would reach the transmitters where they would be blocked by the built-in optical isolators of all transmitters at the hub. Fig. 4.6 illustrates the flow of the downstream and the upstream wavelengths under normal operation.

4.5 Protection mechanism

In case of any single fiber cut between any two ANs, some ANs would not be able to receive their downstream wavelengths while the respective upstream receivers of the affected ANs at the hub would not be able to receive their upstream wavelengths. Such conditions will trigger all the 2×2 optical switches associated with the transceivers designated for the affected ANs at the hub to toggle their switching states automatically, either from bar state to cross state or vice versa. As a result, all the blocked downstream wavelengths can be routed to the affected ANs in an opposite propagating direction along the ring network while all the respective upstream receivers at the hub can still receive a copy of the upstream wavelengths. Fig. 4.7 illustrates the flow of the downstream and the upstream wavelengths when the fiber between AN_1 and AN_2 is broken, as an example. Under this condition, the downstream wavelength for AN_2 (λ_5) could not reach AN_2 via the CCW path. Thus the protection switching at the hub re-routes λ_5 to go along the CW path and reach the downstream receiver at AN_2 via the B-OADM. At the same time, the upstream wavelength λ_7 from AN_2 would reach the respective upstream receiver at the hub via a different path, as illustrated in Fig. 4.7. Note that when there is a single fiber cut between $AN_{N/2}$ and $AN_{N/2+1}$ in an N-node ring network, no protection switching is needed as all of the downstream and the upstream wavelengths could still be routed to their respective receivers in their normal paths. With this proposed protection mechanism, a fast 100% restoration of any single fiber cut in the ring network can be achieved and all protection switching operations are performed at the hub only.

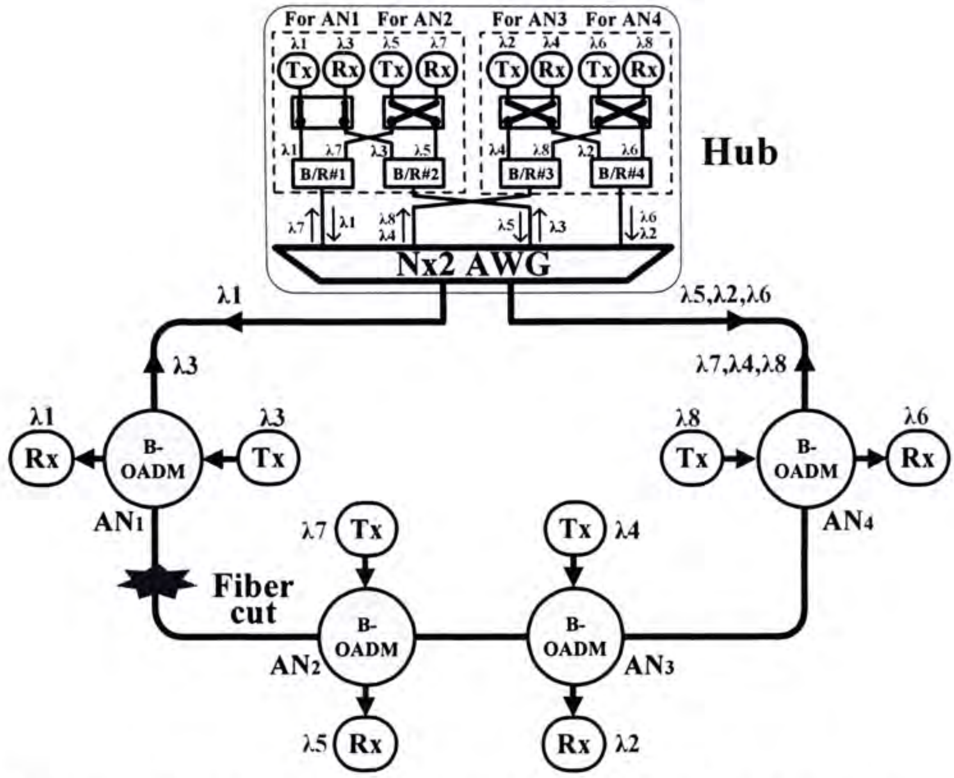

Fig. 4.7 Configuration of the proposed single-fiber bidirectional metro-access network under protection mode. Note: λ_5 (downstream) is re-routed to the clockwise direction of the ring network while λ_7 (upstream) is selected from the counter-clockwise direction.

4.6 Experimental demonstration

In the experiment, we adopted the B-OADM based on a commercially available MZI-FBG, as shown in Fig. 4.4. We first characterized the performance of the proposed B-OADM. The reflectivity of the FBG in the FBG-MZI was 99.94%. The 3-dB bandwidth of the input-drop and input-bypass transfer functions of the B-OADM was around 0.25 nm, which is determined by the grating design and fabrication, as shown in the Fig. 4.8(a) and Fig. 4.8(b), respectively. Thus, the proposed B-OADM is capable of multiplexing/demultiplexing DWDM optical channels with a channel spacing of 0.8 nm. For the dropped signal, there are three types of possible crosstalk. The first one is due to the leakage of the bypass wavelengths (λ_1 to λ_{2N} except λ_k) to the drop port (i.e. from port 1 to 2/3 and from port 4 to 2/3). The port numbers are shown in Fig. 4.4. This type of heterodyne crosstalk was measured to be less than -29 dB, as shown in the Fig. 4.8(c) and could be suppressed by optical filters. The second one is due to the leakage of the dropped wavelength λ_k to the bypass port (i.e. from port 1 to 4 or from port 4 to 1), which is caused by the imperfect reflection of the FBG. This type of crosstalk was measured to be below -30 dB. Since the dropped wavelength λ_k originated from the hub would be transmitted to the AN in either CW or CCW unidirectional way at one time, so the residual dropped signal after passing through the B-OADM would not affect the network performance. The last one is due to the leakage of the dropped wavelength λ_k to the drop port on the other side (i.e. from port 1 to 3 and from port 4 to 2). Although this type of homodyne crosstalk could not filtered off at the receiver, it was measured to be below –40 dB, owing to the interference property of the MZI structure, thus it had negligible influence on the network performance. For the added signal, since it was added and transmitted to the hub in both CW and CCW directions, its performance was sensitive to the reflection at each B-OADM. The crosstalk level of the reflection of the bypass added signals at the B-OADM (e.g. from port 1 to port 1 or from port 4 to port 4) plus the Rayleigh backscattering was measured to be less than -60 dB, so that the transmission performance of the added signal would not be degraded by the crosstalk due to possible reflection and Rayleigh backscattering.

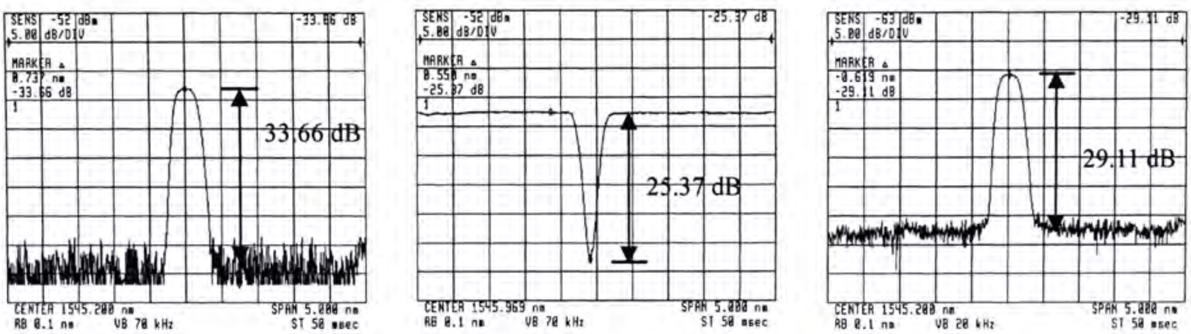

(a) (b) (c)

Fig. 4.8 (a) Input-drop port transfer function of the B-OADM. (b) Input-bypass port transfer function of the B-OADM. (c) Crosstalk level on the dropped signal measured at the port 2 of B-OADM.

The receiver sensitivity (@ BER = 10^{-9}) was also measured as a function of the misalignment of the dropped wavelength channel from the FBG center wavelength, as shown in Fig. 4.9. As another signal was added through two separate optical couplers, the added signals would not affect the signal dropped by the MZI-FBG. It showed that the usable bandwidth (~0.2 nm) was almost the same as the 3-dB bandwidth of the transfer function even with the presence of the added signal. Thus the limit on the usable bandwidth of the conventional configuration of OADM using MZI-FBG for adding and dropping signals at the same time could be alleviated [32].

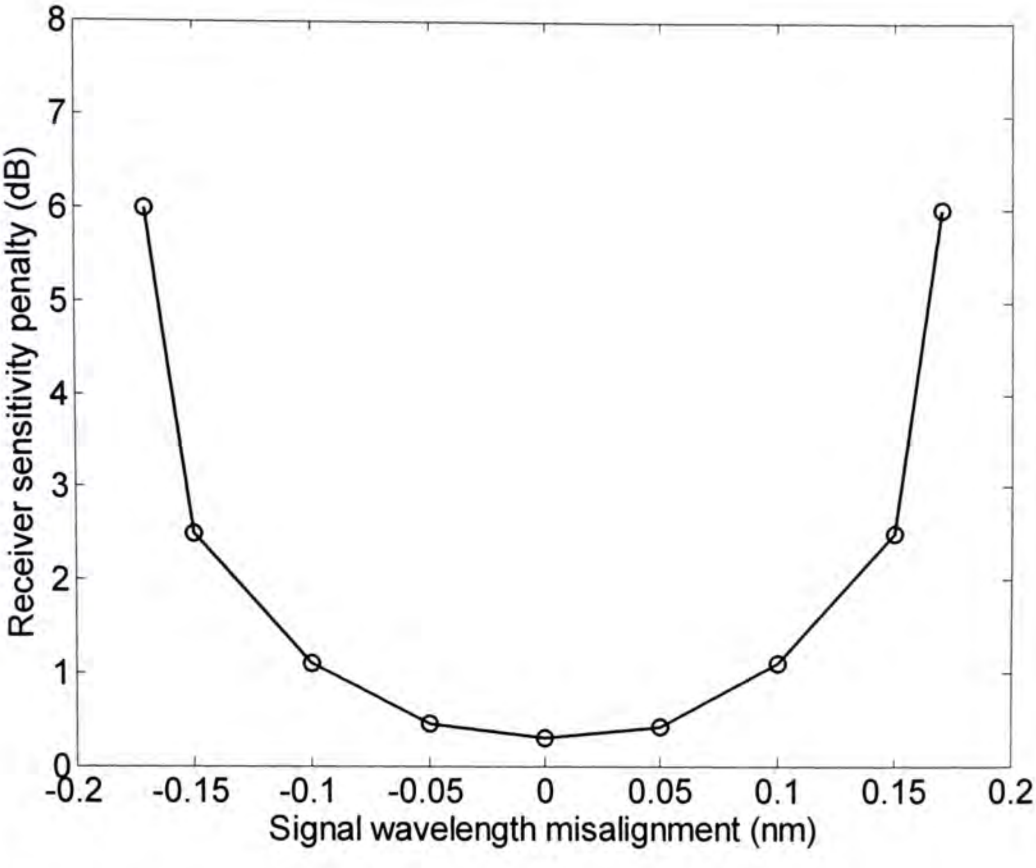

Fig. 4.9 Receiver sensitivity penalty measured as a function of the fluctuation of the dropped wavelength channel.

We have also experimentally demonstrated the proposed network with one hub node and two ANs. A piece of 10-km conventional single-mode fiber (SMF) was used to connect an AN to the hub or the adjacent AN. At the hub, the Blue/Red filters with 18-nm passband at both blue and red bands were used and connected to a 16×16 AWG, with 100-GHz channel spacing and a FSR of 12.8 nm. The output ports 1 and 9 of the AWG were used to connect to the transmission fibers of the ring network. The wavelengths {downstream; upstream} assigned for AN_1 and AN_2 were {λ_1:1545.2 nm; λ_9:1551.6 nm) and {λ_{17}:1568.0 nm; λ_{25}:1574.4 nm), respectively. Note that the two downstream wavelengths were spaced by one FSR of the AWG and so were the upstream wavelengths. All the wavelengths channels were directly modulated at 2.5 Gb/s (PRBS 2^{31-1}) and the output power per channel of the hub was amplified to 0 dBm by EDFA. At the hub, the wavelengths λ_1 was transmitted to AN_1 in CW direction while λ_{17} was transmitted to AN_2 in CCW direction. At the same time, two other wavelengths λ_2 (1546.0 nm) and λ_{18} (1568.8 nm) were transmitted in the CW and CCW direction to simulate the downstream signals for AN_2 and AN_4, respectively. At AN_1, the downstream wavelength λ_1 was dropped by the MZI-FBG at the B-OADM; while the upstream wavelength λ_9 was added and transmitted to the hub in both CW and CCW paths. Similarly, at AN_2, the downstream wavelength λ_{17} was dropped by the MZI-FBG at the B-OADM; while the upstream wavelength λ_{25} was added and received by the APD receivers at the hub. A tap coupler and a monitoring unit were employed in front of each upstream receiver at the hub so as to detect any signal loss due to any possible fiber cut in the network.

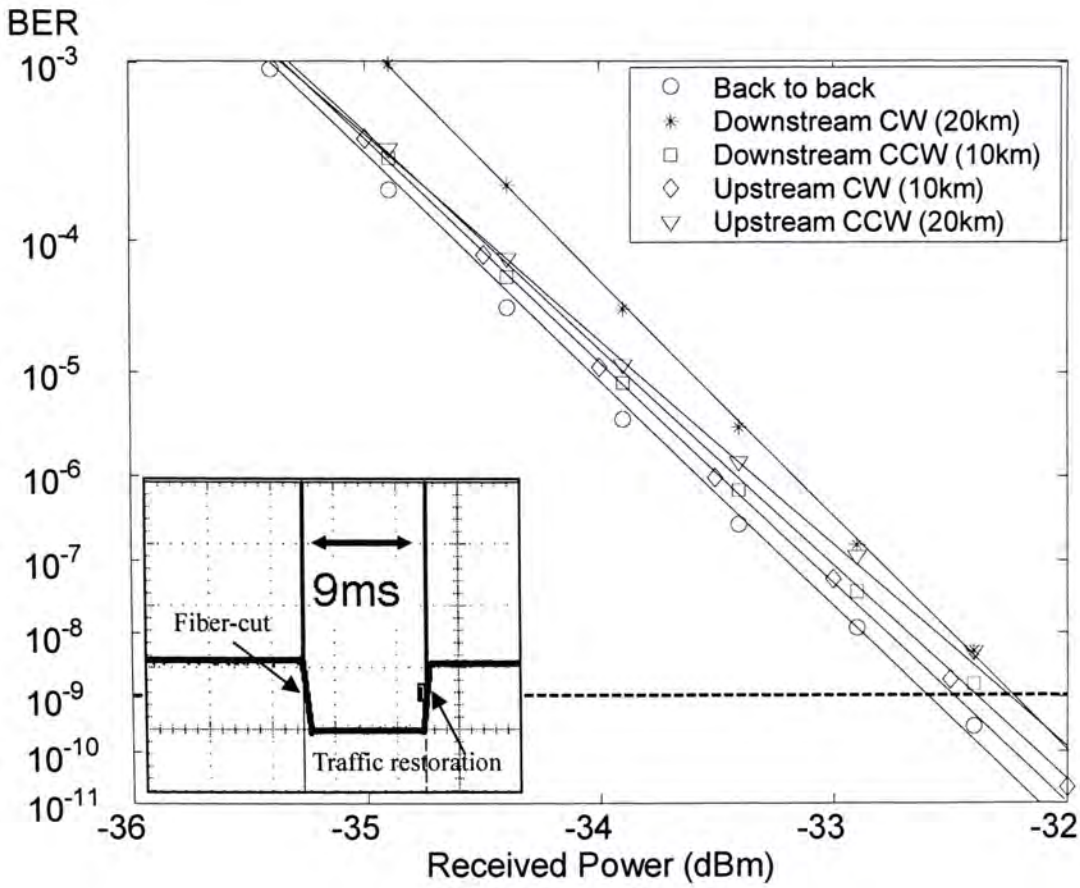

Fig. 4.10 BER measurement of the traffic between the hub node and AN_1 under operation and protection modes. Inset shows the restoration time measurement under the protection mode. CW: clockwise direction; CCW: counter-clockwise direction.

The bit-error-rate (BER) performance of the traffic between the hub and AN_1 under both normal and protection modes were measured and was depicted in Fig. 4.10. In all cases, the measured receiver sensitivities at BER = 10^{-9} were close to each other. The small induced power penalty (<0.5 dB) compared to the back-to-back measurement was due to possible crosstalk of the MZI-FBG at the B-OADM analyzed above and the chromatic dispersion of fiber. Then, the fiber between the hub and AN_1 was disconnected to simulate the fiber cut. The inset of Fig. 4.10 shows the downstream power level measured at the receiver at AN_1. The switching time was measured to be about 9 ms and this corresponds to the network traffic restoration time achieved.

Similar switching waveform was also obtained at the upstream receiver for AN_1 at the hub.

4.7 Optimization of access node

In order to estimate the power budget of the proposed network, we optimize the coupling ratio of the optical couplers for adding upstream signals incorporated at each B-OADM. We assume that the output power per channel of the hub is amplified to 0 dBm by bi-directional EDFA inside the hub, the output power from the transmitter at each AN is 3 dBm, the length of the fiber link between adjacent ANs is 10 km with 2 dB loss, the APD receiver sensitivity is –30 dBm at BER = 10^{-9} at 2.5 Gb/s; and the insertion loss of the MZI-FBG is 0.5 dB. If the coupling ratio of the two couplers for adding upstream signal is x : (1-x), the total insertion loss of the B-OADM at each AN for the bypass, dropped and added signals are $-20\log(x)+0.5$, $-10\log(x)+3.5$ and $-10\log(1-x)+3$ dB respectively. Considering the worst case with N nodes, both the dropped and the added signals pass through (N-1) ANs to reach the AN and the hub respectively, which experience $(-20\log(x)+0.5)\times(N-1)$ dB bypass loss plus $2N$ dB transmission loss. Thus we have the following power budget equations,

$$(-20\log(x)+0.5)\times(N-1)+2N-10\log(x)+3.5=30 \quad \text{for dropped signal}$$

$$(-20\log(x)+0.5)\times(N-1)+2N-10\log(1-x)+3=33 \quad \text{for added signal}$$

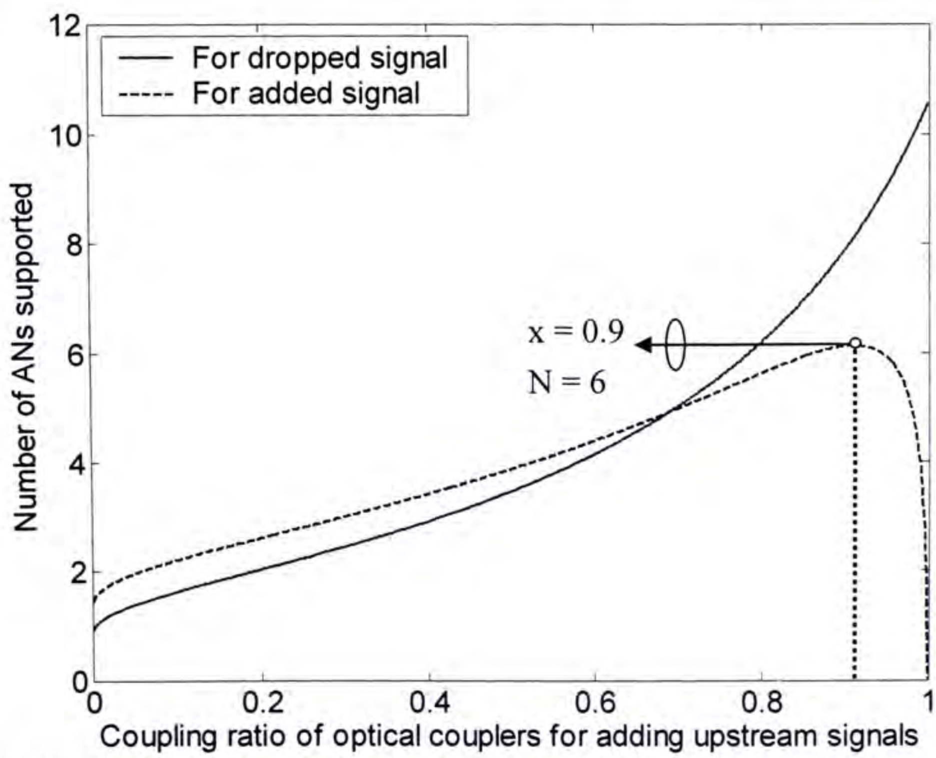

Fig. 4.11 Number of ANs supported with the optimized coupling ratio of the two optical couplers for adding upstream signals in each AN.

The number of ANs supported in the network is plotted as a function of the coupling ratio of the optical couplers for adding upstream signals in the Fig. 4.11. It shows that the maximum $N = 6$ is achieved when $x = 0.9$. Thus, the coupling ratio of the couplers for adding upstream signals is chosen to be 90:10, the proposed network is capable of supporting 6 ANs without any in-line optical amplifiers.

4.8 Scalability

For the scalability of the proposed network, the general hub configuration for N ANs (N is an even number) is shown in the Fig. 4.12. The switches in the first $N/2$ transceivers for AN_1 to $AN_{N/2}$ are configured to bar state while those in the last $N/2$ transceivers for $AN_{N/2+1}$ to AN_N are configured to cross state. Two adjacent transceivers form a group and communicate with their respective ANs, one with odd index B/R#($2i$-1) and the other with even index ($2i$), respectively. In each group, the Blue/Red filter with odd index ($2i$-1) is connected to the i^{th} input ports of the $N\times2$ AWG, which is in the first half of total input ports (i.e. Ports 1 to $N/2$); while the Blue/Red filter with even index ($2i$) is connected to the $(N/2+i)^{\text{th}}$ input ports of the $N\times2$ AWG, which is in the second half of total input ports (i.e. Ports $N/2+1$ to N). The spectral transmission peaks of the two output ports of the AWG are spaced by half of its FSR. Each of these two output ports is connected to the transmission fiber of the ring network in either direction. Besides, in case of the number of ANs in the network is odd, the transceiver unit for AN_N with the dashed box could be removed to support (N-1) ANs.

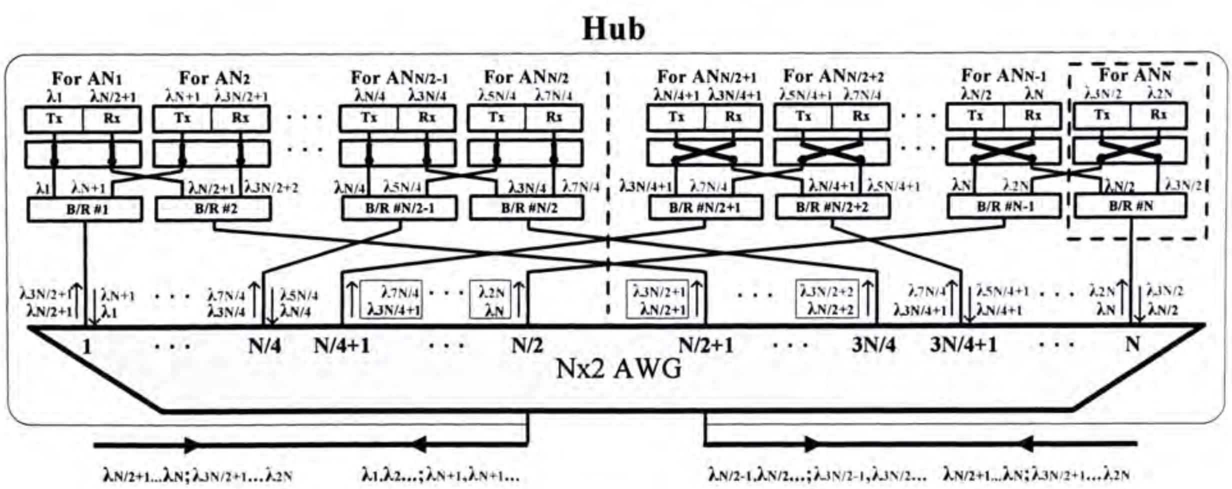

Fig. 4.12 General configuration of the hub node with N ANs in the proposed network.

In order to make the network to support more than 6 ANs, bi-directional in-line optical amplifiers could be used between adjacent ANs. With the commercially available Blue/Red filters, which has 18-nm passband at both blue and red bands, and 100-GHz channel spacing AWG, the proposed network could support at least 32 ANs (16 ANs in each band) considering the imperfect passband transition in the Blue/Red filter. To further increase the network size, the wavelength channels in L band can be further employed with the Blue/Red filters passband covering C+L bands.

4.9 Summary

In this chapter, we have proposed and demonstrated a single-fiber bidirectional WDM SHR for metro-access network with a hub and multiple ANs. By using the proposed alternate-path switching scheme, the proposed network can provide self-healing function without any extra protection fiber. The protection switching is performed at the hub only. Thus, the network reliability can be enhanced in a more cost-effective way. Experiment results showed that a fast restoration time of 9 ms could be achieved under a single fiber failure. Design optimization and scalability of the network have been discussed.

Chapter 5
Self-Healing WDM Mesh Network Architecture for Metro Backbone Networks

5.1 Introduction

Wavelength division multiplexing (WDM) is a promising technology to unleash the enormous bandwidth and greatly increase the system capacity. However, the frequent occurrence of fiber failure may lead to tremendous traffic loss. Thus network survivability becomes a critical concern in network design and management. With the advent of intelligent optical switching, vendors and service providers alike have started to move away from conventional ring-based network architectures because of the poor scalability of interconnected rings and the excessive resource redundancy in ring-based fault management schemes. Instead, they are looking at mesh-based network architectures, which offer restoration using intelligent optical switches.

Nowadays, optical networks are migrating from SONET rings to mesh topology because of the poor scalability of interconnected rings and the excessive resource redundancy in ring-based fault management schemes. Survivable WDM mesh networks have been extensively studied throughout the past decade [33]. Nevertheless, most of the previous work focused on the protection and restoration algorithms implemented in the media access control (MAC) and network layer, which incurred a significant delay caused by the route computation, resource discovery and etc. [34][35][36]. Little work has been done on the physical layer for protection against the fiber failures in optical mesh networks.

In this chapter, we will propose a new protection architecture for mesh metro backbone networks. The network design and the protection strategies under various fiber failure scenarios will be discussed. Besides, the experiment results confirm the feasibility of the proposed network architecture.

5.2 Network architecture and node structure

Fig. 5.1 shows our proposed WDM mesh network, whose topology is similar to a Manhattan-street network [37]. Every two adjacent network nodes are connected by a single piece of fiber. According to the node connectivity, we classify all network nodes into two kinds, namely black nodes and white nodes, in such a way that each black node is connected to four neighboring white nodes, and vice versa, as depicted in Fig. 5.1. The insets of Fig. 5.1 show the proposed wavelength assignment as well as the structure of a network node. Each white node transmits the outgoing data traffic destined to the four connected black nodes on four different wavelengths $\{\lambda_1, \lambda_2, \lambda_3, \lambda_4\}$, respectively. Similarly, each black node transmits the outgoing data traffic destined to the four connected white nodes on another four wavelengths {λ_5, λ_6, λ_7, λ_8}, respectively. The outgoing wavelength channels λ_i ($i \in \{1,2,3,4\}$) and λ_{i+4} from a white node and the adjacent black node, respectively, are transmitted bi-directionally via the same piece of inter-connecting fiber link connecting the output port *i* of both of the white and the black nodes. Moreover, these two wavelength channels (λ_i and λ_{i+4}) are spaced by one free-spectral range (FSR) of the 4×4 array waveguide grating (AWG) employed in every network node. In general, these eight wavelengths (λ_1 to λ_8) are spatially reused over the entire network, as shown in Fig. 5.1.

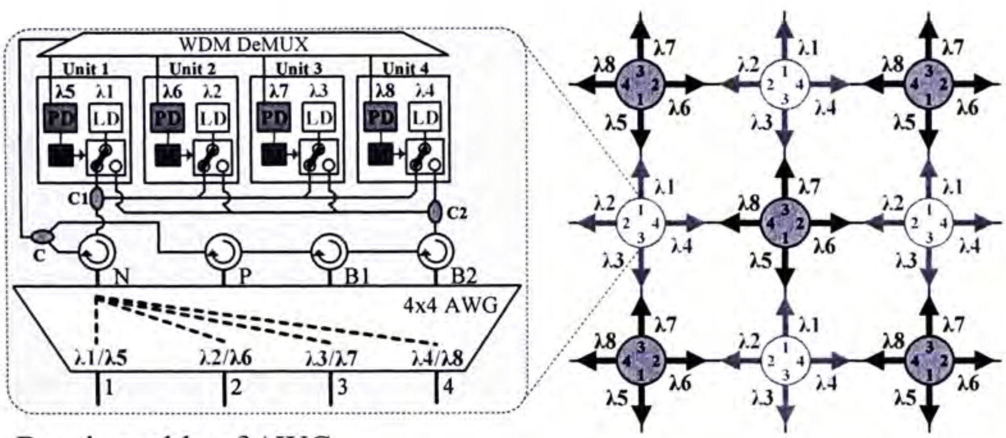

Routing table of AWG

OUT\IN	N	P	B1	B2
1	λ_1,λ_5	λ_4,λ_8	λ_3,λ_7	λ_2,λ_6
2	λ_2,λ_6	λ_1,λ_5	λ_4,λ_8	λ_3,λ_7
3	λ_3,λ_7	λ_2,λ_6	λ_1,λ_5	λ_4,λ_8
4	λ_4,λ_8	λ_3,λ_7	λ_2,λ_6	λ_1,λ_5

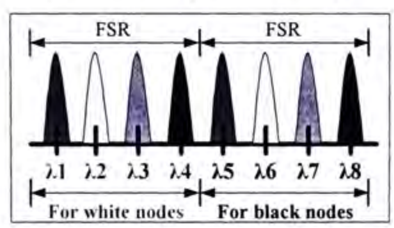

Fig. 5.1 Proposed mesh network with the wavelength assignment plan; FSR: free-spectral range of the AWG; Inset shows the node configuration under normal operation; C: optical coupler; M: monitoring unit.

The inset of Fig. 5.1 shows the structure of a white node, for example, under normal operation. Four transceiver units are incorporated to support the data transmission via the four attached fiber links. Each transceiver emits at λ_i ($i \in \{1,2,3,4\}$) and receives at λ_{i+4}, respectively. The transmitter (LD) in each transceiver is connected to a 1×2 optical switch, which is used to switch the corresponding wavelength either to port *N* (normal mode) or port B2 (protection mode) of the 4×4 AWG, for wavelength routing. Under normal operation, all the optical switches are configured to the left port (as in Fig. 5.1 inset) and the four outgoing wavelength channels {λ_1, λ_2, λ_3, λ_4} are combined by a 4×1 optical coupler (C1) and are routed to port N of the AWG via an optical circulator. The AWG then routes the outgoing wavelengths {λ_1, λ_2, λ_3, λ_4} to their respective output ports, according to the routing table depicted in Fig. 5.1. Each of the four output ports is connected to its respective adjacent black node. At the same time, all of these four output ports also receive wavelength channels $\{\lambda_5, \lambda_6, \lambda_7, \lambda_8\}$ originating from the four connected black nodes. At each output port of the AWG, as the receiving wavelength is spaced an FSR away from the respective outgoing wavelength, all the received wavelengths are routed to port N of the AWG and each of the received wavelengths reaches its respective receiver (PD) via the optical circulator, an optical coupler (C) and a 1×4 WDM demultiplexer. The additional optical circulators located at ports P, B1 and B2 of the AWG are designated for protection mode. On the other hand, a black node has the same structure as a white node except that each of its transceivers, in contrast, emits at λ_{i+4} ($i \in \{1,2,3,4\}$) and receives at λ_i, respectively.

5.3 Protection mechanism

Fig. 5.2 illustrates an example when there is a single fiber link failure between two adjacent nodes. The outgoing wavelength λ_1 from the lower-left white node and also λ_5 from the upper-left black node are affected. As shown in the inset (i), a drastic drop in received power at the monitoring unit (M) of the transceiver unit 1 will be detected. This automatically triggers the optical switch of transceiver unit 1 to switch to the right port. As a result, the wavelength λ_1 destined for the upper-left black node is routed to the port B2 of the 4×4 AWG via a 4×1 optical coupler (C2) and an optical circulator. According to the channel-shifting input-output property of the AWG, as depicted in the routing table of Fig. 5.1, the wavelength λ_1 is routed to the output port 4 of the AWG. As a result, both λ_4 (normal mode) and the re-routed λ_1 (protected mode) are simultaneously transmitted to the output port 4 of the connected lower-right black node, where the received λ_4 is normally routed to its respective receiver; while the received λ_1 is looped back to its output port 3 via ports B2 and B1 of the AWG and the two relevant optical circulators, as illustrated in the inset (ii). In this way, both λ_7 (normal mode) and the re-routed λ_1 (protected mode) are simultaneously transmitted from the output port 3 of the lower-right black node to the output port 3 of the connected upper-right white node, where the received λ_7 is normally routed to its respective receiver; while the received λ_1 is looped back to its output port 2 via ports B1 and P of the AWG and the two relevant optical circulators, as illustrated in the inset (iii). Consequently, both λ_2 (normal mode) and the re-routed λ_1 (protected mode) are simultaneously transmitted from the output port 2 of the upper-right white node to the output port 2 of the connected upper-left black node, where the received λ_2 is normally routed to its respective receiver; while the received λ_1 is also routed to the receiver at its transceiver unit 1 via port P of the AWG, the relevant optical circulator and the WDM demultiplexer, as illustrated in the inset (iv). As a result, λ_1 from the lower-left (white) node can be routed to its destined upper-left (black) node via the two other nodes (lower-right, upper-right) in a counter-clockwise all-optical path.

With the similar protection routing principle, the blocked wavelength λ_5 from the upper-left black node can reach its destined lower-left white node via two other nodes on the left side in a counter-clockwise all-optical path, as shown in Fig. 5.2. In general, this protection scheme applies to any four network nodes (two black and two white) which are interconnected in a quadrilateral loop, in the whole WDM mesh network. With this novel protection mechanism, the affected traffic can be restored promptly without any optical-electrical-optical (O/E/O) conversion nor disturbance to the existing traffic.

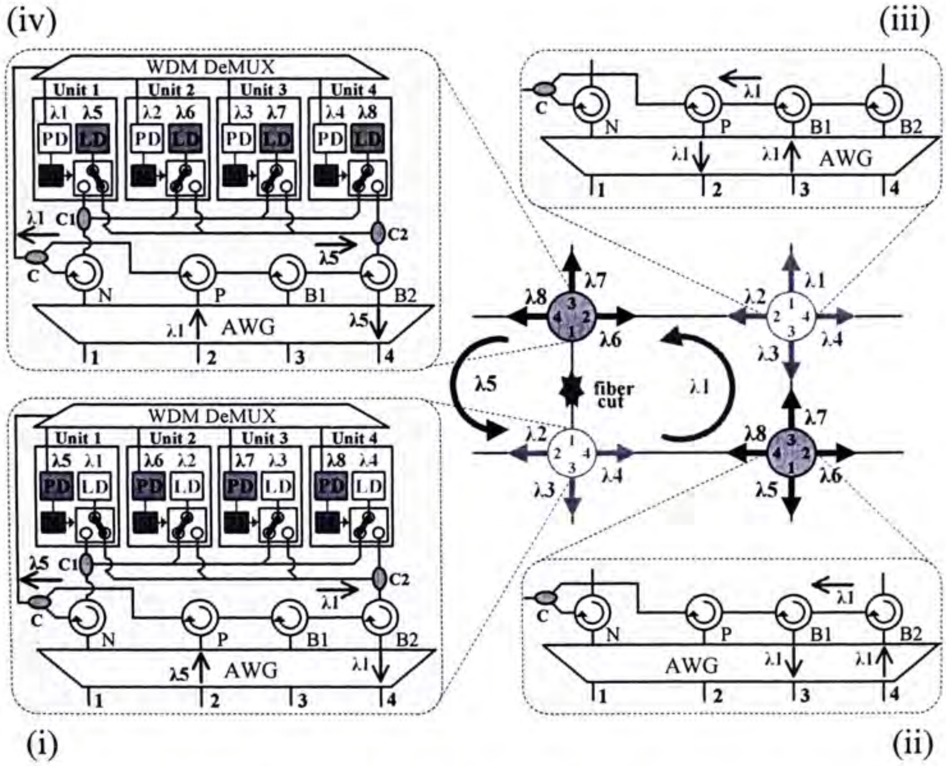

Fig. 5.2 Node configurations under single fiber link failure

Besides, if there exists multiple fiber link failures, the proposed mesh protection architecture can still be able to protect and restore the affected traffic using the proposed scheme, provided that no more than one fiber link failure occurs in a quadrilateral loop as shown in the Fig. 5.3. This scheme is named as all-optical deflection routing for link restoration.

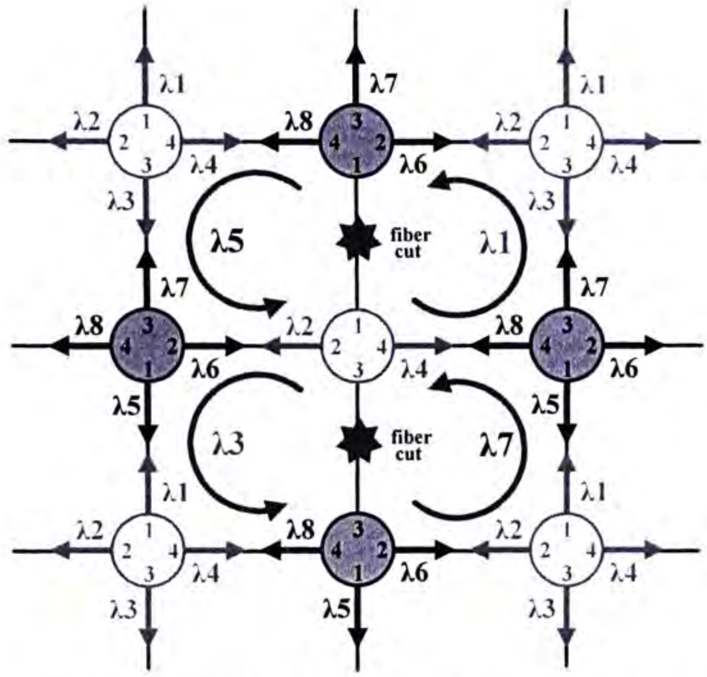

Fig. 5.3 Multiple fiber link failures protection

5.4 Experimental demonstration

The transmission performance and the protection switching of our proposed network were experimentally investigated, using the setup shown in the Fig. 5.4. A 16×16 AWG, with 100-GHz channel spacing and a free-spectral range (FSR) of 12.8 nm, was used. The input ports {4, 8, 12, 16} are chosen as the ports {N, P, B1, B2} to simulate the switching function of the 4×4 AWG. Moreover, each of the output ports {1, 5, 9, 13} of the AWG is connected to the output port with the same index of another AWG by a piece of 10-km standard single-mode fiber (SMF) to simulate four network nodes in a quadrilateral loop. In the upper node (as black nodes), the wavelength λ_5 (1544.0nm) was directly modulated with 2.5-Gb/s 2^{31-1} PRBS data and was combined with another three CW light {λ_6 (1547.2nm), λ_7 (1550.4nm), λ_8 (1553.6nm)} for transmission. While the wavelength λ_1 (1531.2nm) originated from the lower node (as white nodes) was also directly modulated with 2.5-Gb/s 2^{31-1} PRBS data. An optical bandpass filter (BPF) was used in front of each receiver as the demultiplexer to select the corresponding receiving wavelength. The flow path of the wavelengths λ_1 and λ_5 under normal operation is marked with the boxes in Fig. 5.4. The 1×2 optical switches and optical circulators were incorporated in each node to simulate the routing paths of the wavelengths λ_1 and λ_5 under protection mode as shown in the Fig. 5.4. The optical power of the received signal at each transceiver unit was monitored. The single fiber link failure was simulated by intentionally disconnect the fiber connections between the two output ports 1 of the AWGs and the results proved the effectiveness of proposed scheme for link restoration. The bit-error-rate (BER) performance under both the normal and the protection path were measured and was depicted in Fig. 5.5. The induced power penalty (<1dB) compared to the back-to-back measurement was due to fiber chromatic dispersion of the directly modulated wavelength channels.

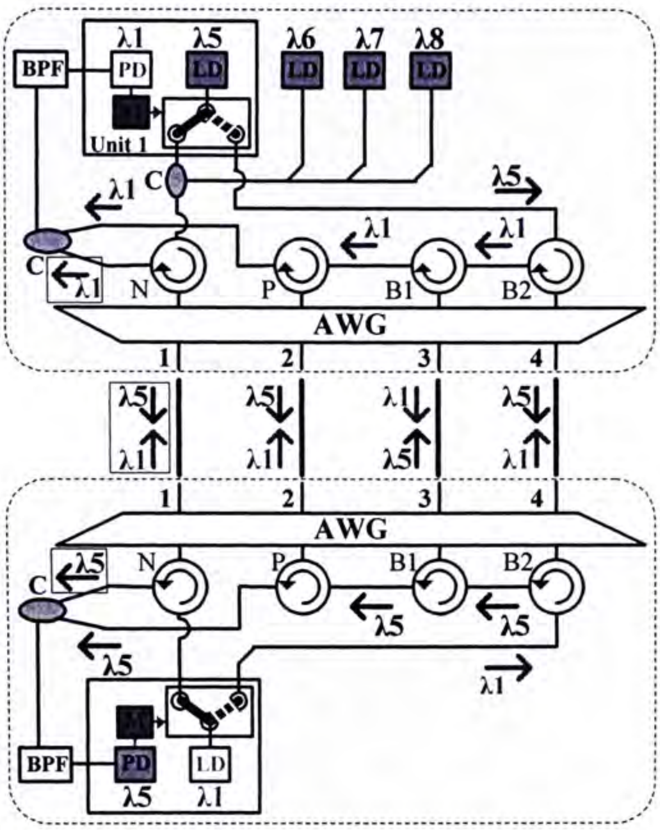

Fig. 5.4 Experimental setup. BPF: bandpass filter; M: power monitor; C: optical coupler; LD: laser diode; PD: photodiode. Note: the solid switching state and the wavelength paths in boxes are for normal mode; while the dotted switching state and the unboxed wavelength paths are for protection mode.

The switching time or the restoration time in case of simulated fiber cut was also measured. The result was shown in the inset of Fig. 5.5. The waveform showed the signal measured at the monitoring unit in the affected transceiver unit. The switching time was measured to be about 3 ms and this corresponded to the network traffic restoration time achieved.

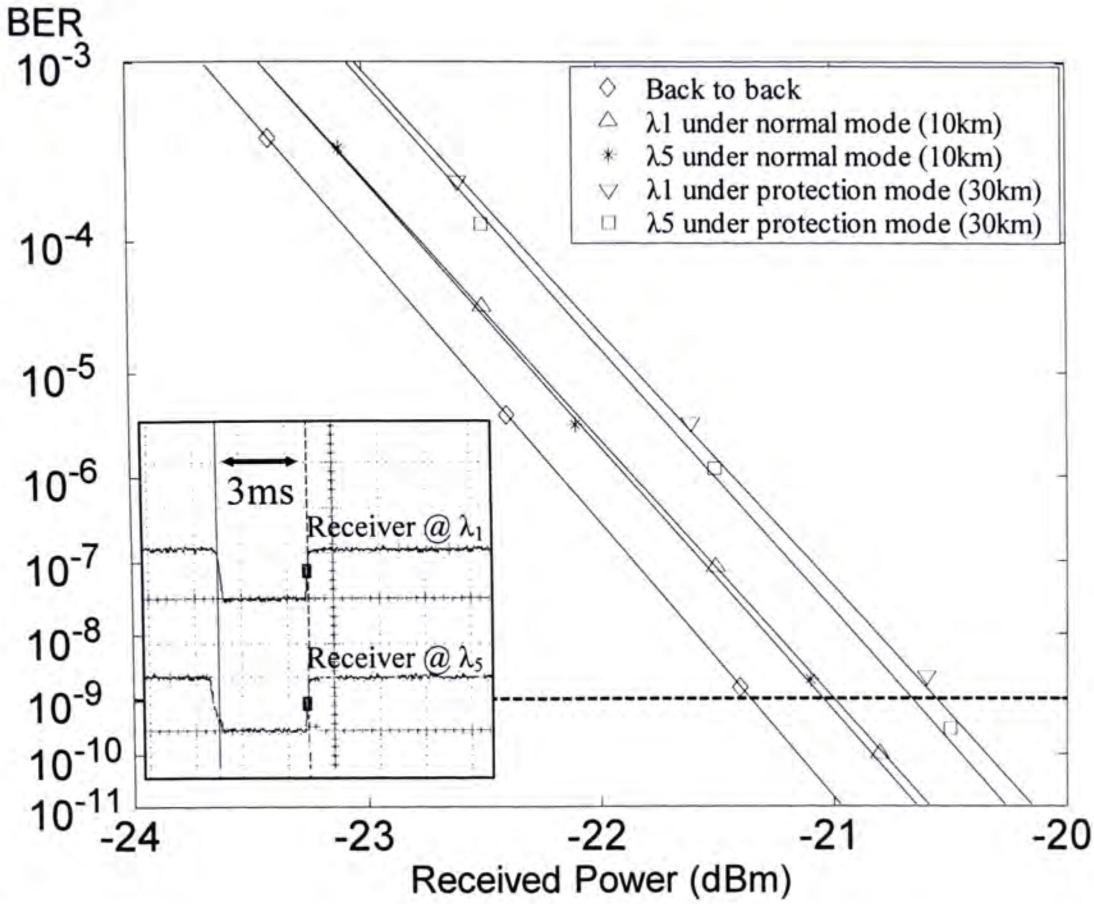

Fig. 5.5 BER measurement of the traffic between two adjacent nodes under operation and protection modes. Inset shows the switching time measurement under the protection mode.

5.5 Summary

In this chapter, we have proposed a new WDM mesh network with a novel all-optical deflection routing scheme for link restoration. With a unified network node design and the proposed wavelength assignment plan, the proposed scheme can be applied to a large-scale WDM mesh network. Fast protection and traffic restoration are achieved in the physical layer. Hence, a reliable and scalable WDM mesh metro backbone network can be realized.

Chapter 6
Summary and Future Works

6.1 Summary of the Thesis

The objective of this thesis is to design and investigate novel self-healing network architectures for multiwavelength optical metropolitan area networks and access networks to enhance network reliability and simplify fault management.

In chapter 1, the evolution of optical network was reviewed. In particular, the challenge of network reliability in mulitwavelength optical metro and access networks was presented.

In chapter 2, previous self-healing network architectures for optical metro/access networks were reviewed. We reviewed conventional protection architectures on ATM-PON (G.983.1), as well as the recent work on protection architectures for WDM-PON. After that, we reviewed traditional self-healing rings in the metro access and metro backbone networks.

In chapter 3, the self-healing network architectures for multiwavelength access networks were discussed. We proposed two self-healing network architectures for WDM-PON. Based on the wavelength routing property of the AWG in the RN, any fiber link failure in the network can be protected and affected traffic can be restored promptly.

In chapter 4, the self-healing network architecture for multiwavelength metro access networks was discussed. We proposed a single-fiber bi-directional self-healing metro access ring network with simple and low-cost bi-directional OADMs. Based on the alternate-path switching mechanism, the proposed self-healing metro access network is cost-effective and reliable.

In chapter 5, the self-healing network architecture for multiwavelength metro backbone networks was discussed. The poor scalability of interconnected SONET rings and the excessive resource redundancy in ring-based fault management schemes were presented. Then we proposed a self-healing mesh network architectures for metro backbone networks. Based on the all-optical deflection routing scheme, a superior high-speed physical-layer protection mechanism can be achieved.

6.2 Future Works

In the future, we will explore the self-healing network architecture with more functions in the optical metro/access networks deeper. In terms of the access network, the reconfigurable architecture with protection capability should be investigated. Also the scalability of optical access network with different topologies needs to be studied. In terms of the metro access network, seamless connection between the access and metro backbone network should be further investigated. Wavelength routing and processing at the access node and hub can be further improved. In terms of metro backbone network, scalability, robustness and topology variations with minimized cost are some stringent requirements. We will also study the possibility of applying those physical-layer-protection concepts in wide-area backbone network with irregular topology. We expect that could be a promising technology in the future.

LIST OF PUBLICATIONS

[1] X.F. Sun, Z.X. Wang, C.K. Chan, L.K. Chen, "A Novel Star-Ring Protection Architecture Scheme for WDM Passive Optical Access Networks", *IEEE/OSA Optical Fiber Communication Conference, OFC 2005, Paper JWA53, Anaheim, California, USA, Mar. 2005.*

[2] X.F. Sun, Z.X. Wang, C.K. Chan, C.L. Lin, L.K. Chen, "A Single-Fiber Bi-directional Self-Healing WDM Metro-Ring Network with Bi-directional OADM", *European Conference on Optical Communications, ECOC 2005, Paper We4.P.41, Glasgow, United Kingdom, Sep. 2005.*

[3] X.F. Sun, C.K. Chan, L.K. Chen, "A Survivable WDM PON with Alternate-Path Switching", *IEEE/OSA Optical Fiber Communication Conference, OFC 2006, Paper JThB71, Anaheim, California, USA, Mar. 2006*

[4] X.F. Sun, C.K. Chan, L.K. Chen, "A Survivable WDM PON Architecture with Centralized Alternate-Path Protection Switching for Traffic Restoration", *IEEE Photonics Technology Letters, vol. 18, no. 3, Mar. 2006.*

[5] X.F. Sun, Z.X. Wang, C.K. Chan, C.L. Lin, L.K. Chen, "A Single-Fiber Bi-directional WDM Self-Healing Ring Network with Bi-directional OADM for Metro-Access Applications", submitted to *IEEE Journal on Selected Areas in Communications (JSAC) of "Optical Communications and Networking (OCN)".*

[6] Z.X. Wang, X.F. Sun, C.L. Lin, C.K. Chan, L.K. Chen, "A Novel Surveillance Scheme for Passive Optical Networks Using Spectral Analysis", *European Conference on Optical Communications (ECOC), Paper We4.P.142, Stockholm, Sweden, Sep. 2004.*

[7] Z.X. Wang, X.F. Sun, C.L. Lin, C.K. Chan, L.K. Chen, "A Novel Centrally Controlled Protection Scheme for Traffic Restoration in WDM Passive Optical Networks", *IEEE Photonics Technology Letters, vol. 17, no. 3, pp. 717-719, Mar. 2005.*

[8] C.M. Lee, X.F. Sun, C.K. Chan, and L.K. Chen, "A Single-Fiber Bi-directional Self-Healing WDM Mesh Network with All-Optical Cyclic Deflection Routing for Link Restoration", *IEEE Photonics Technology Letters, vol. 17, no. 11, Nov. 2005.*

[9] Q.G. Zhao, X.F. Sun, Y.C. Ku, C.K. Chan, L.K. Chen, "A Novel Internetworking Scheme for WDM Passive Optical Network based on Remodulation Technique", *IEEE/OSA Optical Fiber Communication Conference, OFC 2006, Paper JThB67, Anaheim, California, USA, Mar. 2006.*

REFERENCES

[1] "Big fiber deployments–undersea cable projects," *ATM News Digest*, December 1998.

[2] L. Chen, X. Bao "Polarization-dependent loss-induced pulse narrowing in birefringent optical fiber with differential group delay," *IEEE/OSA J. Lightwave Technol.*, Vol.18, No5, pp.665-667, 2000.

[3] "Upstart carriers seize an ocean of opportunity," *Fiber Systems*, Vol.3, No.5, June 1999.

[4] J. Chesnoy, O. Gautheron, L. Le Gourrierec, V. Lemaire, "Evolution of WDM submarine systems towards terabit/s integrated networks," *Alcatel Telecommunication Review*, 3rd quarter 1998.

[5] "Submarine networks: snapshots," *Fiber Systems*, Vol.3, No.5, June 1999.

[6] C. DeCusatis et al, "Handbook of fiber optic data communication," *Academic Press*, 1998.

[7] R. Sharma, "Demystifying metropolitan optical networks," *IEEE/OSA J. Lightwave Technol.*, Vol.16, No.10, Sept 1999.

[8] "The emerging digital economy," *U.S. Department of Commerce Publication*, April 1998. (http://www.ecommerce.gov/emerging.htm).

[9] C. Decusatis, "Optical data communication: fundamentals and future directions," *Optical Engineering*, Vol.37, No12, pp.3082-3099, 1998.

[10] N. Golmie, D. T. Ndousse, D. H. Su, "A differentiated optical services model for WDM networks," *IEEE Communications Magazine*, Feb 2000.

[11] "Vendors plan a 10Gbit/s future for Ethernet," *Fiber Systems*, Vol.3, No.7, September 1999.

[12] http://grouper.ieee.org/groups/802/3/ae/index.html

[13] ITU-T Recommendation G.983.1, *Broadband optical access systems based on Passive Optical Networks (PON)*, 1998

[14] W. P. Lin et al, "A star-bus-ring architecture for DWDM/SCM passive optical networks", *Lasers and Electro-Optics, CLEO/Pacific Rim*, Volume 2, page 580-581, July, 2001.

[15]T. J. Chan, et al, "A self-protected architecture for wavelength division multiplexed passive optical networks," *IEEE Photonic Technology Letters*, vol. 15, pp. 1660-1662, November 2003.

[16]C. M. Lee, T. J. Chan, C. K. Chan, L. K. Chen, C.L. Lin, "A group protection architecture (GPA) for traffic restoration in multi-wavelength passive optical networks," *European Conference on Optical Communications ECOC*, Paper Th2.4.2, Rimini, Italy, Sept 2003.

[17]Wu, T.-H., Kolar, D.J., Cardwell, R.H., "Survivable network architectures for broad-band fiber optic networks: model and performance comparison," *IEEE/OSA J. Lightwave Technol.,* vol. 6, no. 11, pp. 1698-1709, November, 1988.

[18]S. B. Park, C. H. Lee, "Bidirectional WDM self-healing ring network composed of add fiber and drop fiber," *Electron. Lett.,* vol. 37, pp. 446–448, March 2001.

[19]S. B. Park, C. H. Lee, S. G. Kang, S. B. Lee, "Bidirectional WDM self-healing ring network for hub/remote nodes," *IEEE Photon. Technol. Lett.*, vol. 15, pp. 1657-1659, November 2003.

[20]Y. Joo, G. Lee, R. K. Kim, S. Park, K. Song, Koh, J.; S. Hwang, Y. Oh, and Shim, C., "1-fiber WDM self-healing ring with bidirectional optical add/drop multiplexers," *IEEE Photon. Technol. Lett.*, vol. 16, pp. 683-685, February 2004.

[21]R. Ramaswami, et al., "Optical networks: a practical perspective", 2nd Edition, *Morgan Kauffman*

[22]Y.-K. M. Lin and D. R. Spears, "Passive optical subscriber loops with multi-access," *IEEE/OSA J. Lightwave Technol.,* vol. 7, no. 11, pp. 1769-1777, November, 1989.

[23]I. M. McGregor, G. J. Semple, and G. Nicholson, "Implementation of a TDM passive optical network for subscriber loop applications," *IEEE/OSA J. Lightwave Technol.,* vol. 7, no. 11, pp. 1752-1758, Nov. 1989.

[24]M. J. M. van Vaalen, "Asynchronous transfer mode transmission on a passive optical home network," *17th International Television Symp.Tech. Exhibition,* pp. 97-107, June 1991.

[25]D. W. Faulkner, et al, "Optical networks for local loop application," *IEEE/OSA J. Lightwave Technol.*, vol. 7, pp. 1741-1751, 1989.

[26]S. S. Wagner and H. L. Lemberg, "Technology and system issues for WDM-based fiber loop architecture," *IEEE/OSA J. Lightwave Technol.*, vol. 7, pp. 1759-1768, November, 1989.

[27] Wu, T.-H., Kolar, D.J., Cardwell, R.H., "Survivable network architectures for broad-band fiber optic networks: model and performance comparison," *IEEE/OSA J. Lightwave Technol.*, vol.6, pp. 1698-1709, November, 1988.

[28] C. H. Kim, C.-H. Lee, and Y. C. Chung, "Bidirectional WDM selfhealing ring network based on simple bidirectional add–drop amplifier modules," *IEEE Photon. Technol. Lett.*, vol. 10, pp. 1340–1342, September 1998.

[29] V. Tholey et al., "Demonstration of WDM survivable unidirectional ring network using tunable channel dropping receivers," *Electron. Lett.*, vol. 30, pp. 1323–1324, Aug. 1994.

[30] A. F. Elrefaie, "Multiwavelength survivable ring network architectures," *Proceedings of IEEE International Conference on Communications (ICC)*, vol. 2, pp.1245-1251, Geneva, May 1993.

[31] F. Bilodeau, D. C. Johnson, S. Theriault, B. Malo, J. Albert, and K. O. Hill, "An all-fiber dense wavelength division multiplexer/demultiplexer using photoimprinted Bragg gratings," *IEEE Photon. Technol. Lett.*, vol. 7, no. 4, pp. 388-390, 1995.

[32] Pedersen, R.J.S., and Jorgensen, B.F., "Impact of coherent crosstalk on usable bandwidth of a grating-MZI based OADM," *IEEE Photon. Technol. Lett*, vol. 10, pp. 558-560, April 2003.

[33] J. Zhang, B. Mukherjee, "A review of fault management in WDM mesh networks: basic concepts and research challenges," *IEEE Network*, vol. 18, issue: 2, pp. 41-48, Mar-Apr 2004.

[34] S. Ramamurthy, L. Sahasrabuddhe, and B. Mukherjee, "Survivable WDM mesh networks," *IEEE/OSA J. Lightwave Tech.*, vol. 21, pp. 870-883, Apr 2003.

[35] G. Ellinas, A. Hailemariam, and T. E. Stern, "Protection cycles in mesh WDM networks," *IEEE J. Selected Areas in Commun.*, vol. 18, pp. 1924-37, Oct 2001.

[36] R. Ramamurthy et al., "Capacity performance of dynamic provisioning in optical networks," *IEEE/OSA J. Lightwave Tech.*, vol. 19, pp. 40-48, Jan 2001.

[37] N.F. Maxemchuk, "The Manhattan Street Network," *Proceedings of IEEE Globecom*, pp. 255-261, 1985.